

Genes Involved in Sister Chromatid Separation and Segregation in the Budding Yeast *Saccharomyces cerevisiae*

Sue Biggins,¹ Needhi Bhalla,² Amy Chang, Dana L. Smith³ and Andrew W. Murray²

Department of Physiology, University of California, San Francisco, California 94143

Manuscript received March 5, 2001

Accepted for publication June 28, 2001

ABSTRACT

Accurate chromosome segregation requires the precise coordination of events during the cell cycle. Replicated sister chromatids are held together while they are properly attached to and aligned by the mitotic spindle at metaphase. At anaphase, the links between sisters must be promptly dissolved to allow the mitotic spindle to rapidly separate them to opposite poles. To isolate genes involved in chromosome behavior during mitosis, we microscopically screened a temperature-sensitive collection of budding yeast mutants that contain a GFP-marked chromosome. Nine *LOC* (loss of cohesion) complementation groups that do not segregate sister chromatids at anaphase were identified. We cloned the corresponding genes and performed secondary tests to determine their function in chromosome behavior. We determined that three *LOC* genes, *PDS1*, *ESP1*, and *YCS4*, are required for sister chromatid separation and three other *LOC* genes, *CSE4*, *IPL1*, and *SMT3*, are required for chromosome segregation. We isolated alleles of two genes involved in splicing, *PRP16* and *PRP19*, which impair α -tubulin synthesis thus preventing spindle assembly, as well as an allele of *CDC7* that is defective in DNA replication. We also report an initial characterization of phenotypes associated with the *SMT3/SUMO* gene and the isolation of *WSSI*, a high-copy *smt3* suppressor.

ACCURATE cell division depends upon the proper segregation of chromosomes into daughter cells. When chromosomes replicate during S phase, cohesion between the sister chromatids is established and must be maintained while chromosomes condense and align on the mitotic spindle. Chromosomes attach to the mitotic spindle by their kinetochores, specialized protein structures that are assembled on centromeric DNA sequences. Once all the chromosomes are correctly aligned on the mitotic spindle, the cohesion between sister chromatids must dissolve promptly at anaphase to allow the sister chromatids to rapidly segregate to opposite poles of the mitotic spindle. Accurate chromosome segregation depends on precisely timed sister chromatid separation (the destruction of the linkage between sisters) and chromosome segregation (the movement of the separated sister chromatids to opposite poles of the spindle).

A number of proteins involved in sister chromatid cohesion and separation have been identified (for review, see NASMYTH *et al.* 2000). A conserved complex,

cohesin, is required to establish and maintain the link between sisters. The cohesin complex contains two homologous ATP binding proteins, Smc1 and Smc3, in addition to the Scc3/Irr1 and Scc1/Mcd1 proteins (GUACCI *et al.* 1997; MICHAELIS *et al.* 1997). The budding yeast cohesins associate with chromosomes during DNA replication and remain bound until the metaphase to anaphase transition (MICHAELIS *et al.* 1997; UHLMANN and NASMYTH 1998). At the onset of anaphase, the Esp1 protein cleaves Scc1/Mcd1p, leading to sister chromatid separation (UHLMANN *et al.* 1999, 2000). Prior to anaphase, Esp1p is inactive due to binding of the Pds1 protein, which inhibits its activity (CROSK *et al.* 1998). Anaphase is initiated by the ubiquitin-mediated proteolysis of Pds1p, which is triggered by activating the cyclosome/APC complex (COHEN-FIX *et al.* 1996). In addition to the cohesins, additional proteins have been identified that are required to establish cohesion during DNA replication (SKIBBENS *et al.* 1999; TOTH *et al.* 1999; CROSK *et al.* 2000).

After establishing cohesion, chromosomes must condense to ensure accurate chromosome transmission (for review, see HIRANO 2000). Condensation is regulated at least in part by the condensins, a conserved complex related to the cohesin complex (HIRANO and MITCHISON 1994; HIRANO *et al.* 1997). The budding yeast condensin complex contains two related Smc protein homologs, Smc2 and Smc4, as well as three regulatory proteins, Brn1, Ycs4, and Ycs5 (STRUNNIKOV *et al.* 1995; FREEMAN *et al.* 2000; LAVOIE *et al.* 2000; OUSPENSKI *et al.* 2000). The condensin complex is essential for chro-

Corresponding author: Sue Biggins, Division of Basic Sciences, Fred Hutchinson Cancer Research Ctr., 1100 Fairview Ave. N., A2-168, Seattle, WA 98109. E-mail: sbiggins@fhcrc.org

¹ *Present address:* Division of Basic Sciences, Fred Hutchinson Cancer Research Ctr., Seattle, WA 98109.

² *Present address:* Department of Molecular and Cell Biology, Harvard University, Cambridge, MA 02138.

³ *Present address:* Department of Biochemistry and Biophysics, University of California, San Francisco, CA 94143.

mosome condensation in higher eukaryotes. In budding yeast, it is essential for condensation of the repetitive ribosomal DNA (rDNA; FREEMAN *et al.* 2000). The yeast condensin complex localizes to the nucleolus and is required to segregate the rDNA at mitosis. There is a link between budding yeast chromosome condensation and cohesion because two proteins required for cohesion, Pds5 and Scc1/Mcd1, have defects in condensation (GUACCI *et al.* 1997; HARTMAN *et al.* 2000).

Chromosome segregation also depends on mitotic spindle and kinetochore functions (for review, see PIDOUX and ALLSHIRE 2000). A protein complex called CBF3, which contains four components (Skp1p, Ndc10p, Ctf13p, and Cep3p), assembles onto budding yeast centromeric DNA and is essential for kinetochore function (LECHNER and CARBON 1991; SORGER *et al.* 1995; STEMMANN and LECHNER 1996; KAPLAN *et al.* 1997). In addition to CBF3, the yeast kinetochore contains homologs of higher eukaryotic centromere proteins such as the Cse4, Mif2, and Ipl1 proteins (MELUH and KOSHLAND 1995, 1997; MELUH *et al.* 1998; S. BIGGINS and A. W. MURRAY, unpublished data). Cse4p is a conserved Histone H3 variant that is the homolog of CENP-A in mammalian cells and is thought to form a specialized nucleosome structure at the kinetochore (STOLER *et al.* 1995). Cse4p localizes to yeast kinetochores and *cse4* mutants have defective kinetochore function and altered centromeric chromatin structure (STOLER *et al.* 1995; MELUH *et al.* 1998). The Mif2 protein, a homolog of CENP-C in higher eukaryotes, is also required for kinetochore function and localizes to kinetochores (BROWN *et al.* 1993; MELUH and KOSHLAND 1995, 1997). The *IPL1* gene encodes a conserved protein kinase called *Aurora* in higher eukaryotes that regulates kinetochore function in budding yeast (FRANCISCO *et al.* 1994; BIGGINS *et al.* 1999). Ipl1p phosphorylates the CBF3 component Ndc10p *in vitro*, suggesting that it may regulate kinetochore function at least in part via Ndc10p phosphorylation (BIGGINS *et al.* 1999). The fidelity of kinetochore function is monitored by the spindle assembly checkpoint, which arrests cells in metaphase until defects in chromosome attachment are corrected (for review, see GARDNER and BURKE 2000).

Smt3/SUMO is a conserved ubiquitin-like protein that is post-translationally conjugated to substrate proteins (for review, see SAITOH *et al.* 1997). In higher eukaryotes, a number of potential substrates for SUMO have been identified, such as RanGAP1 (MATUNIS *et al.* 1996; MAHAJAN *et al.* 1997). In budding yeast, *SMT3* is an essential gene that was isolated as a high-copy suppressor of a temperature-sensitive *mif2* kinetochore mutant (MELUH and KOSHLAND 1995). Smt3p conjugates to three of the five mitotic septins that localize to the bud neck and are required for cytokinesis (JOHNSON and BLOBEL 1999; TAKAHASHI *et al.* 1999). However, the essential functions of *SMT3* are not mediated through septin conjugation because mutations that abolish this

conjugation are not lethal (JOHNSON and BLOBEL 1999). Smt3p localizes to the nucleus in addition to the bud neck, suggesting it has a second nuclear function, consistent with its isolation as a high-copy suppressor of a *mif2* mutation.

We report the identification of mutants that affect chromosome separation and segregation, using strains whose chromosome IV is marked by the binding of a green fluorescent protein (GFP)-Lac repressor fusion to a tandem array of Lactose operators. We isolated temperature-sensitive (ts) mutants and examined them microscopically to identify mutants that appear to be defective in the separation of sister chromatids at anaphase [*loss of cohesion (LOC)*]. We identified 9 *LOC* complementation groups and used secondary tests to determine whether they affect either sister chromatid separation or segregation. In addition, we provide an initial characterization of *smt3* phenotypes in budding yeast and the isolation of a high-copy suppressor of the *smt3* mutant named *WSS1*.

MATERIALS AND METHODS

Microbial techniques: Media and genetic and microbial techniques were essentially as described (SHERMAN *et al.* 1974; ROSE *et al.* 1990). All experiments where cells were released from a G1 arrest were carried out by adding 1 $\mu\text{g}/\text{ml}$ α -factor at the permissive temperature (23°) for 4 hr, washing cells twice in α -factor-free media, and resuspending them in pre-warmed media at 37°. When cells started to bud, α -factor was added back to prevent cells from entering the next cell cycle. All experiments were repeated at least twice with similar results and at least 100 cells were counted at each time point. Stock solutions of inhibitors were stored at -20°: 30 mg/ml benomyl (DuPont, Wilmington, DE) in DMSO, 10 mg/ml nocodazole (Sigma, St. Louis) in DMSO, 10 mg/ml α -factor (Bio-Synthesis, Lewisville, TX) in DMSO, and 5 mg/ml doxycycline (Sigma) in methanol. For benomyl/nocodazole experiments, cells were released into 30 $\mu\text{g}/\text{ml}$ benomyl and 15 $\mu\text{g}/\text{ml}$ nocodazole at 37°. For the *CSE4* repression experiments, 5 $\mu\text{g}/\text{ml}$ doxycycline was added when cells were released from G1. To visualize sister chromatids, copper sulfate was added to media at a final concentration of 0.25 mg/ml to induce the GFP-lacI fusion protein that is under the control of the copper promoter.

Yeast strain constructions: Yeast strains are listed in Table 1 and were constructed by standard genetic techniques. Diploids were isolated on selective media at 23° and subsequently sporulated at 23°. The galactose-inducible nondegradable mitotic cyclin (*pGAL- Δ 176-CLB2*) that is contained in some strains is not expressed in glucose media (data not shown). The strains XL1-Blue and DH5 α were used for all bacterial manipulations. The strain used for the screen was constructed by first deleting the *LYS2* gene in SBY3 by integrating pAR88 (gift of Adam Rudner) digested with *Xba*I. The *URA3* gene was then selected against on 5-fluoroorotic acid plates to obtain SBY181, which contains an unmarked *lys2 Δ* . SBY181 was subsequently integrated with the following plasmids, respectively, to generate SBY215: *pGAL- Δ 176-CLB2:LYS2* (pSB102) that was digested with *Bsp*EI, *pCUP-GFP12-LacI:HIS3* that was digested with *Nhe*I (pSB116; BIGGINS *et al.* 1999), and *lacO:TRP1* (256 lactose operators on plasmid pAFS52; STRAIGHT *et al.* 1996) that was digested with *Eco*RV. All *mad2 Δ* *loc* and *cdc23-1* *loc* double mutants were constructed by crosses. The intronless tubulin

TABLE 1
Yeast strains used in this study

Strain	Genotype
SBY3	MATa <i>ura3-1 leu2,3-112 his3-11 trp1-1 ade2-1 can1-100 bar1Δ</i>
SBY15	MATa/MATx <i>ura3-1/ura3-1 leu2,3-112/leu2,3-112 his3-11/his3-11 trp1-1/trp1-1 ade2-1/ade2-1 can1-100/can1-100 bar1Δ/bar1Δ</i>
SBY153	MATa <i>ura3-1 leu2,3-112 his3-11:pCUP1-GFP12-lacI12:HIS3 trp1-1:lacO:TRP1 ade2-1 can1-100 bar1Δ lys2Δ prp19-153</i>
SBY155	MATx <i>ura3-1 leu2,3-112 his3-11:pCUP1-GFP12-lacI12:HIS3 trp1-1:lacO:TRP1 ade2-1 can1-100 barΔ lys2Δ:pGAL-Δ176-CLB2:LYS2 prp19-153</i>
SBY181	MATa <i>ura3-1 leu2,3-112 his3-11 trp1-1 ade2-1 can1-100 bar1Δ lys2Δ</i>
SBY186	MATa <i>ura3-1 leu2,3-112 his3-11:pCUP1-GFP12-lacI12:HIS3 trp1-1:lacO:TRP1 ade2-1 can1-100 bar1Δ lys2Δ <i>cdc23-1</i></i>
SBY214	MATa <i>ura3-1 leu2,3-112 his3-11:pCUP1-GFP12-lacI12:HIS3 trp1-1:lacO:TRP1 ade2-1 can1-100 bar1Δ lys2Δ</i>
SBY215	MATa <i>ura3-1 leu2,3-112 his3-11:pCUP1-GFP12-lacI12:HIS3 trp1-1:lacO:TRP1 ade2-1 can1-100 bar1Δ lys2Δ:pGAL-Δ176-CLB2:LYS2</i>
SBY288	MATx <i>ura3-1 leu2,3-112 his3-11:pCUP1-GFP12-lacI12:HIS3 trp1-1:lacO:TRP1 ade2-1 can1-100 bar1Δ lys2Δ [pRS316]</i>
SBY322	MATa <i>ura3-1 leu2,3-112 his3-11:pCUP1-GFP12-lacI12:HIS3 trp1-1:lacO:TRP1 ade2-1 can1-100 bar1Δ lys2Δ <i>ipb1-521</i></i>
SBY323	MATa <i>ura3-1 leu2,3-112 his3-11:pCUP1-GFP12-lacI12:HIS3 trp1-1:lacO:TRP1 ade2-1 can1-100 bar1Δ lys2Δ <i>cse4-323</i></i>
SBY327	MATx <i>ura3-1 leu2,3-112 his3-11:pCUP1-GFP12-lacI12:HIS3 trp1-1:lacO:TRP1 ade2-1 can1-100 bar1Δ lys2Δ <i>cse4-327</i></i>
SBY329	MATa <i>ura3-1 leu2,3-112 his3-11:pCUP1-GFP12-lacI12:HIS3 trp1-1:lacO:TRP1 ade2-1 can1-100 bar1Δ lys2Δ <i>cse4-327</i></i>
SBY331	MATa <i>ura3-1 leu2,3-112 his3-11:pCUP1-GFP12-lacI12:HIS3 trp1-1:lacO:TRP1 ade2-1 can1-100 bar1Δ lys2Δ <i>smt3-331</i></i>
SBY333	MATa <i>ura3-1 leu2,3-112 his3-11:pCUP1-GFP12-lacI12:HIS3 trp1-1:lacO:TRP1 ade2-1 can1-100 bar1Δ lys2Δ:pGAL-Δ176-CLB:LYS2 <i>smt3-331</i></i>
SBY355	MATa <i>ura3-1 leu2,3-112 his3-11:pCUP1-GFP12-lacI12:HIS3 trp1-1:lacO:TRP1 ade2-1 can1-100 bar1Δ lys2Δ <i>cdc7-355</i></i>
SBY358	MATx <i>ura3-1 leu2,3-112 his3-11:pCUP1-GFP12-lacI12:HIS3 trp1-1:lacO:TRP1 ade2-1 can1-100 barΔ lys2Δ:pGAL-GALΔ176-CLB2:LYS2 <i>cdc7-355</i></i>
SBY382	MATa <i>ura3-1 leu2,3-112 his3-11:pCUP1-GFP12-lacI12:HIS3 trp1-1:lacO:TRP1 ade2-1 can1-100 bar1Δ lys2Δ:pGAL-Δ176-CLB2:LYS2 ESP1-HA3:URA3:HA3</i>
SBY458	MATa <i>ura3-1 leu2,3-112 his3-11:pCUP1-GFP12-lacI12:HIS3 trp1-1:lacO:TRP1 ade2-1 can1-100 bar1Δ mad2::URA3 <i>esp1-478</i></i>
SBY468	MATa <i>ura3-1 leu2,3-112 his3-11:pCUP1-GFP12-lacI12:HIS3 trp1-1:lacO:TRP1 ade2-1 can1-100 bar1Δ lys2Δ <i>mad2::URA3</i></i>
SBY473	MATa <i>ura3-1 leu2,3-112 his3-11:pCUP1-GFP12-lacI12:HIS3 trp1-1:lacO:TRP1 ade2-1 can1-100 bar1Δ lys2Δ <i>cdc21-1 prp19-153</i></i>
SBY478	MATa <i>ura3-1 leu2,3-112 his3-11:pCUP1-GFP12-lacI12:HIS3 trp1-1:lacO:TRP1 ade2-1 can1-100 bar1Δ lys2Δ <i>esp1-478</i></i>
SBY482	MATx <i>ura3-1 leu2,3-112 his3-11:pCUP1-GFP12-lacI12:HIS3 trp1-1:lacO:TRP1 ade2-1 can1-100 bar1Δ lys2Δ <i>esp1-478</i></i>
SBY516	MATa/MATx <i>ura3-1/ura3-1 leu2,3-112/leu2,3-112 his3-11/pCUP1-GFP12-lacI12:HIS3/his3-11:pCUP1-GFP12-lacI12:HIS3 trp1-1:lacO:TRP1/trp1-1:lacO:TRP1 <i>ade2-1/ade2-1 can1-100/can1-100 bar1Δ/bar1Δ lys2Δ/lys2Δ:pGAL-Δ176-CLB2:LYS2</i></i>
SBY528	MATx <i>ura3-1 leu2,3-112 his3-11:pCUP1-GFP12-lacI12:HIS3 trp1-1:lacO:TRP1 ade2-1 can1-100 bar1Δ lys2Δ <i>pds1-176</i></i>
SBY530	MATa <i>ura3-1 leu2,3-112 his3-11:pCUP1-GFP12-lacI12:HIS3 trp1-1:lacO:TRP1 ade2-1 can1-100 bar1Δ lys2Δ <i>top2-4 [pRS316]</i></i>
SBY567	MATa <i>ura3-1 leu2,3-112 his3-11:pCUP1-GFP12-lacI12:HIS3 trp1-1:lacO:TRP1 ade2-1 can1-100 bar1Δ lys2Δ <i>mad2::URA3 smt3-331</i></i>
SBY571	MATa <i>ura3-1 leu2,3-112 his3-11:pCUP1-GFP12-lacI12:HIS3 trp1-1:lacO:TRP1 ade2-1 can1-100 bar1Δ lys2Δ <i>prp19-153 rad9::LEU2</i></i>
SBY572	MATa <i>ura3-1 leu2,3-112 his3-11:pCUP1-GFP12-lacI12:HIS3 trp1-1:lacO:TRP1 ade2-1 can1-100 bar1Δ lys2Δ <i>mad2::URA3 rad9::LEU2</i></i>
SBY575	MATa <i>ura3-1 leu2,3-112 his3-11 trp1-1 ade2-1 can1-100 bar1Δ CSE4:pGAL-CSE4-myc13::URA3::KAN</i>
SAB597	MATa/MATx <i>ura3-1/ura3-1 leu2,3-112/leu2,3-112 his3-11/pCUP1-GFP12-lacI12:HIS3/his3-11:pCUP1-GFP12-lacI12:HIS3 trp1-1:lacO:TRP1/trp1-1:lacO:TRP1 <i>ade2-1/ade2-1 can1-100/can1-100 bar1Δ/bar1Δ lys2Δ/lys2Δ:pGAL-Δ176-CLB2:LYS2 CSE4/cse4::KAN</i></i>
SBY599	MATa/MATx <i>ura3-1/ura3-1 leu2,3-112/leu2,3-112 his3-11/pCUP1-GFP12-lacI12:HIS3/his3-11:pCUP1-GFP12-lacI12:HIS3 trp1-1:lacO:TRP1/trp1-1:lacO:TRP1 <i>ade2-1/ade2-1:pTET-CSE4:ADE2 can1-100/can1-100 bar1Δ/bar1Δ lys2Δ/lys2Δ:pGAL-Δ176-CLB2:LYS2 CSE4/cse4::KAN</i></i>
SBY601	MATa <i>ura3-1 leu2,3-112 his3-11:pCUP1-GFP12-lacI12:HIS3 trp1-1:lacO:TRP1 ade2-1:pTET-CSE4:ADE2 can1-100 bar1Δ lys2Δ <i>cse4::KAN</i></i>
SBY626	MATa <i>ura3-1 leu2,3-112 his3-11:pCUP1-GFP12-lacI12:HIS3 trp1-1:lacO:TRP1 ade2-1:pTET-CSE4:ADE2 can1-100 bar1Δ lys2Δ <i>cse4::KAN</i></i>
SBY639	MATa <i>ura3-1 leu2,3-112 his3-11 trp1-1 ade2-1 can1-100 bar1Δ pGAL-HA3-SMT3:HIS3</i>
SBY640	MATa/MATx <i>ura3-1/ura3-1 leu2,3-112/leu2,3-112 his3-11/his3-11 trp1-1/trp1-1 ade2-1/ade2-1 can1-100/can1-100 bar1Δ/bar1Δ SMT3/pGAL-HA3-SMT3:HIS3</i>
SBY696	MATa <i>ura3-1 leu2,3-112 his3-11:pCUP1-GFP12-lacI12:HIS3 trp1-1:lacO:TRP1 ade2-1 can1-100 bar1Δ lys2Δ <i>smt3-331 [pSB254, 2μ WSS1, URA3]</i></i>

(continued)

TABLE 1
(Continued)

Strain	Genotype
SBY710	MATa <i>ura3-1 leu2,3-112 his3-11:pCUP1-GFP12-lacI12:HIS3 trp1-1:lacO:TRP1 ade2-1 can1-100 bar1Δ lys2Δ smt3-331</i> [pSB254]
SBY712	MATa <i>ura3-1 leu2,3-112 his3-11:pCUP1-GFP12-lacI12:HIS3 trp1-1:lacO:TRP1 ade2-1 can1-100 bar1Δ lys2Δ prp16-176</i>
SBY713	MATa <i>ura3-1 leu2,3-112 his3-11:pCUP1-GFP12-lacI12:HIS3 trp1-1:lacO:TRP1 ade2-1 can1-100 bar1Δ lysΔ ipi1-182</i>
SBY740	MATa <i>ura3-1 leu2,3-112 his3-11:pCUP1-GFP12-lacI12:HIS3 trp1-1:lacO:TRP1 ade2-1 can1-100 bar1Δ lys2Δ mad2::URA3 prp19-153</i>
SBY754	MATa/MATα <i>ura3-1/ura3-1 leu2,3-112/leu2,3-112 his3-11:pCUP1-GFP12-lacI12:HIS3/his3-11:pCUP1-GFP12-lacI12:HIS3 trp1-1:lacO:TRP1/trp1-1:lacO:TRP1 ade2-1/ade2-1 can1-100/can1-100 bar1Δ/bar1Δ lys2Δ/lys2Δ:pGAL-Δ176-CLB2:LYS2 WSS1/uss1::KAN</i>
SBY755	MATa <i>ura3-1 leu2,3-112 his3-11:pCUP1-GFP12-lacI12:HIS3 trp1-1:lacO:TRP1 ade2-1 can1-100 bar1Δ lys2Δ:pGAL-Δ176-CLB2:LYS2 uss1::KAN</i>
SBY760	MATa <i>ura3-1 leu2,3-112 his3-11:pCUP1-GFP12-lacI12:HIS3 trp1-1:lacO:TRP1 ade2-1 can1-100 bar1Δ lys2Δ PDS1:PDS1-myc18:LEU2</i>
SBY761	MATa/MATα <i>ura3-1/ura3-1 leu2,3-112/leu2,3-112 his3-11:pCUP1-GFP12-lacI12:HIS3/his3-11:pCUP1-GFP12-lacI12:HIS3 trp1-1:lacO:TRP1/trp1-1:lacO:TRP1 ade2-1/ade2-1 can1-100/can1-100 bar1Δ/bar1Δ lys2Δ/lys2Δ:pGAL-Δ176-CLB2:LYS2 SMT3/pGAL-HA3-SMT3:HIS3 WSS1/WSS1-myc13:KAN</i>
SBY804	MATa <i>ura3-1 leu2,3-112 his3-11:pCUP1-CUP1-GFP12-lacI12:HIS3 trp1-1:lacO:TRP1 ade2-1 can1-100 bar1Δ lys2Δ mad2::URA3 pds1-176</i>
SBY805	MATa <i>ura3-1 leu2,3-112 his3-11:pCUP1-GFP12-lacI12:HIS3 trp1-1:lacO:TRP1 ade2-1 can1-100 bar1Δ lys2Δ mad2Δ ycs4-1 hml::LEU2</i>
SBY808	MATa <i>ura3-1 leu2,3-112:TUB1(in):LEU2 his3-11:pCUP1-GFP12-lacI12:HIS3 trp1-1:lacO:TRP1 ade2-1 can1-100 bar1Δ lys2Δ cdc23-1</i> [pSB273]
SBY809	MATa <i>ura3-1 leu2,3-112:TUB1(in):LEU2 his3-11:pCUP1-GFP12-lacI12:HIS3 trp1-1:lacO:TRP1 ade2-1 can1-100 bar1Δ lys2Δ cdc23-1 prp16-176</i> [pSB273]
SBY817	MATa <i>ura3-1 leu2,3-112 his3-11:pCUP1-GFP12-lacI12:HIS3 trp1-1:lacO:TRP1 ade2-1 can1-100 bar1Δ lys2Δ cdc23-1</i>
SBY828	MATa <i>ura3-1 leu2,3-112 his3-11:pCUP1-GFP12-lacI12:HIS3 trp1-1:lacO:TRP1 ade2-1 can1-100 bar1Δ lys2Δ ycs4-1</i>
SBY830	MATa <i>ura3-1 leu2,3-112 his3-11:pCUP1-GFP12-lacI12:HIS3 trp1-1:lacO:TRP1 ade2-1 can1-100 bar1Δ lys2Δ pds1-176</i>
SBY833	MATa <i>ura3-1 leu2,3-112 his3-11:pCUP1-GFP12-lacI12:HIS3 trp1-1:lacO:TRP1 ade2-1 can1-100 bar1Δ lys2Δ mad2::URA3 prp16-176</i>
SBY837	MATa <i>ura3-1 leu2,3-112 his3-11:pCUP1-GFP12-lacI12:HIS3 trp1-1:lacO:TRP1 ade2-1 can1-100 bar1Δ lys2Δ cdc23-1 prp16-176</i>
SBY840	MATa <i>ura3-1 leu2,3-112 his3-11:pCUP1-GFP12-lacI12:HIS3 trp1-1:lacO:TRP1 ade2-1 can1-100 bar1Δ lys2Δ mad2Δ prp19-153 rad9::LEU2</i>
SBY849	MATa <i>ura3-1 leu2,3-112 his3-11:pCUP1-GFP12-lacI12:HIS3 trp1-1:lacO:TRP1 ade2-1 can1-100 bar1Δ lys2Δ mad2Δ rad9::LEU2</i>
SBY850	MATa <i>ura3-1 leu2,3-112:TUB1(in):LEU2 his3-11:pCUP1-GFP12-lacI12:HIS3 trp1-1:lacO:TRP1 ade2-1 can1-100 bar1Δ lys2Δ cdc23-1 prp19-153</i> [pSB273]
RA5 ^a	MATα <i>ura3-1 leu2,3-112 his3-11 trp1-1 ade2-1 can1-100 gln4::LEU2</i>
YS78-2 ^b	MATa <i>ura3-1 leu2,3-112 his3-11 trp1-1 ade2-1 can1-100 lys2 prp16::LYS2 prp16-2:HIS3</i>
UCC712 ^c	MATα <i>ura3Δ0 leu2Δ0 his3Δ200 trp1Δ63 ade2Δ::hisG lys2Δ0 met15Δ0 sir1::URA3</i>
NBY302	MATa <i>ura3-1 leu2,3-112 his3-11:pCUP1-GFP12-lacI12:HIS3 trp1-1:lacO:TRP1 ade2-1 can1-100 bar1Δ lys2Δ:pGAL-Δ176-CLB2:LYS2 YSC4-HA3:URA3:HA3</i>
NBY290	MATα <i>ura3-1 leu2,3-112 his3-11:pCUP1-GFP12-lacI12:HIS3 trp1-1:lacO:TRP1 ade2-1 can1-100 bar1Δ lys2Δ ycs4-1 hml::LEU2</i>

All strains are isogenic with the W303 background. Plasmids are indicated in brackets. All strains were constructed for this study unless indicated.

^a Doug Kellogg (UC Santa Cruz).

^b Christine Guthrie (UC, San Francisco).

^c Dan Gottschling (FHRC).

strains were constructed by integrating pSB273 (*TUB1 in*) that had been digested with *Afl*III into SBY186, SBY837, and SBY473 to create SBY808, SBY809, and SBY850, respectively. A strain containing *pGAL-HA3-SMT3* was constructed by an *in vivo* PCR integration method. Primers SB47 (5'-GGA/CAG/AAG/GAC/CCA/GTT/CAG/TTC/TAG/TTT/TAC/AAA/TAA/ATA/CAC/GAG/CGG/AAT/TCG/AGC/TCG/TTT/AAA/C-3') and SB48 (5'-TTC/TGG/CTT/GAC/CTC/TGG/CTT/AGC/TTC/TTG/ATT/GAC/TTC/TGA/GTC/CGA/CAT/GCA/CTG/AGC/AGC/GTA/ATC/TG-3') were used to PCR amplify DNA from plasmid pFA6a-His3MX6-pGAL1-3HA (LONGTINE *et al.* 1998). The PCR product was transformed into diploid strain SBY15 to generate SBY640, which was subsequently sporulated in the presence of galactose to generate a haploid containing *pGAL-HA3-SMT3* (SBY639). A strain containing the *YSC4-HA3* was created by PCR integration. Primers LOC7-3 (5'-GTC/ACT/GCA/TTA/TTG/GAG/CAA/GGT/TTC/CAA/GGT/TGT/ATC/CGC/AAA/AGA/AAG/GGA/ACA/AAA/GCT/GG-3') and LOC7-4 (5'-TAA/TAA/CAT/ATA/ATA/TAA/AAC/GGA/AGA/AAC/GGG/TAA/ACG/TCA/GTT/CGA/TTA/CTA/TAG/GGC/GAA/TTG/G-3') were used to PCR amplify DNA from plasmid RTK (gift of Rachel Kulberg), which was integrated into SBY215 to create NBY302. A *wss1Δ* strain was generated by the PCR integration method. Primers SB118 (5'-GTA/ACA/ACG/CAT/ATT/TTG/AAG/ATA/TTC/TAA/ATA/AGA/GAG/ATT/GAT/TAC/GGA/TCC/CCG/GGT/TAA/TTA/A-3') and SB120 (5'-ACA/TTT/ACC/ATA/CTT/ATA/ATT/TTC/GAG/TTC/TTC/GCT/GTG/GAC/AAG/AGA/TTA/TCG/ATG/AAT/TCG/AGC/TCG/TT-3') were used to PCR amplify DNA from plasmid pFA6a-kanMX6 (LONGTINE *et al.* 1998), which was subsequently transformed into SBY516 to generate SBY754. This strain was sporulated to generate *wss1Δ* haploid strain SBY755.

We used a *cse4Δ* strain that was kept alive by a doxycycline-repressible *CSE4* gene for the analysis of sister chromatid separation in a *mad2Δ cse4* double mutant. This was required because of difficulty arresting the *cse4* mutant strains with α -factor. To construct this strain, we first deleted *CSE4* in a diploid strain by the PCR integration method. Primers SB67 (5'-CAG/AAG/AAG/GAC/TGA/ATA/TAG/AAA/GAA/TAC/TAA/TAT AAC/ATA/ATC/CGG/ATC/CCC/GGG/TTA/ATT/AA-3') and SB64 (5'-CCG/AAA/AAG/GGA/AAA/ATC/GGC/TCC/AGC/CCT/GAA/GCA/CAA/ATA/TCA/CTA/TCG/ATG/AAT/TCG/AGC/TCG/TT-3') were used to PCR amplify pFA6a-kanMX6 (LONGTINE *et al.* 1998) and the PCR product was transformed into SBY516 to generate strain SBY597. This strain was transformed with pSB233, a plasmid containing doxycycline-repressible *CSE4*, which had been digested with *Afl*III. The resulting strain, SBY599, was sporulated to generate a haploid *cse4Δ* strain (SBY601) covered by the repressible *CSE4*, which was then crossed to SBY468. The resulting diploid was sporulated to isolate the *cse4Δ mad2Δ* double mutant (SBY626). When analyzed by Western blotting, there is no detectable Cse4 protein in SBY626 after treatment with doxycycline for 1 hr (data not shown). For the *cse4-327 cdc23-1* experiment, we used *GFP-TUB1* (pAFS125, gift of Aaron Straight) to visualize spindles because a large number of cells lysed during the indirect immunofluorescence procedure.

Isolation of *loc* mutants: A temperature-sensitive bank of yeast mutants was generated as follows. Strain SBY215 was mutagenized with EMS or UV to 50% killing as described (ROSE *et al.* 1990). Mutagenized cells were plated at the permissive temperature (23°) until colonies formed and then replica printed to the nonpermissive temperature (37°). After 1 day at 37°, plates were scored and putative *ts* mutants were isolated

from a plate maintained at 23° and retested at 37° for growth. Mutant strains were subsequently colony purified and retested twice at 37°. Finally, mutants that did not grow on glycerol as the sole carbon source were eliminated to ensure the mutants were not petites. We isolated 2000 *ts* mutant strains from ~800,000 mutagenized strains.

We directly screened each *ts* mutant strain by microscopy to identify the *loc* phenotype. Microtiter dishes were inoculated from fresh patches of cells that were grown on plates at 23°. The microtiter dishes were shifted to 37° for 4 hr and placed on ice while we directly screened the cells by microscopy for GFP signals. We isolated 283 potential mutants out of the 2000 *ts* strains in this primary screen. We next screened the mutants for sister chromatid separation at anaphase. Nondestructible *C1b2p* was overexpressed in the 283 mutants by shifting cells to 37° for 2 hr and then adding galactose to 2% final concentration for an additional 2 hr. Cells were screened by microscopy for a qualitative defect of 50% or less sister chromatid separation in the large-budded cells. A total of 52 mutants passed this test and were then analyzed for a cell division cycle (*cdc*) phenotype. Cells were shifted to 37° for 4 hr and quantified for the number of large-budded cells. The remaining 48 mutant strains containing <70% large-budded cells in the population were then tested for rapid death, an indication of chromosome breakage, at 37° and rescue of this death by benomyl/nocodazole. Asynchronously growing mutant strains were shifted to 37° in the presence or absence of benomyl/nocodazole and plated for viability at 23° 0, 2, and 4 hr later. Eleven mutant strains that decreased viability by 50% or greater during the 4-hr temperature shift but showed an increased viability in the presence of benomyl/nocodazole were retained.

The 11 *loc* mutant strains were crossed to SBY238, the resulting diploids were tested for the *ts* phenotype, and all were recessive. They were then backcrossed once to SBY238 to generate *MAT α* and *MAT α* strains that were used to generate diploids for complementation testing, which determined there were nine complementation groups. They were then backcrossed four times to SBY215 and retested for the lack of a *cdc* phenotype and for sister chromatid separation by microscopy. We did not repeat the other secondary tests on the backcrossed strains.

***loc* mutant cloning and linkage tests:** The *loc* mutants were cloned by complementation of the *ts* phenotype using a centromere-based yeast genomic library as described (HARDWICK and MURRAY 1995). Plasmid DNA from colonies that grew at 37° was isolated and transformed into bacteria. The DNA was retransformed into each corresponding *loc* mutant and plasmids that conferred temperature resistance were sequenced. We identified the complementing region of the clones by subcloning various regions of the plasmids and testing for complementation of the *ts* phenotype.

We performed linkage tests to ensure that the cloned genes corresponded to the mutations and not suppressing genes. For *loc1*, SBY575 containing *pGAL-CSE4-myc13:URA3* was crossed to SBY323 and SBY327 and in 18 tetrads the *URA3* marker always segregated away from the *loc1* *ts* phenotype. The *loc2* linkage tests were previously described (BIGGINS *et al.* 1999). For *loc3*, we determined that the *smt3-331* *ts* phenotype is linked to the *GIN4* gene by crossing an *smt3-331* mutant strain to a *GIN4*-marked strain (RA5; gift of Doug Kellogg, UC Santa Cruz, CA). For *loc4*, pTW004 containing the *CDC7* gene marked with *URA3* (gift of J. Li, UC San Francisco) was digested with *Bam*HI and integrated into SBY181. The resulting strain was crossed to SBY358, the diploids were sporulated, and in 22 tetrads the *loc4* *ts* phenotype always segregated away from the *URA3* marker. For *loc5*, we crossed SBY712 to UCC712 (gift of D. Gottschling, FHCRC) that contains a *URA3*-marked *SIR1*

gene and found that *URA3* always segregated away from the *loc5* ts phenotype in 20 tetrads. We also determined that the *loc5-1* allele does not complement a *prp16-2* allele (YS78-2; gift of C. Guthrie, UC San Francisco). For the *loc6* linkage test, the *loc6* allele (SBY528) was crossed to a strain with a marked *PDS1-myc18:LEU2* allele (SBY760) and in 22 tetrads the ts phenotype always segregated away from the *LEU2* marker. For the *loc7* linkage test, NBY302 containing *URA3*-marked *YSC4-HA3* was crossed to NBY290 and the resulting diploid was sporulated. Out of 22 tetrads dissected, the *URA3* marker always segregated away from the *loc7* ts phenotype. For the *prp19* linkage test, pSB194 was digested with *Bgl*II and integrated into SBY214. The resulting strain was crossed to SBY155 and 22 tetrads were analyzed, and we determined that the ts phenotype always segregated away from the marked plasmid. In addition, we determined that the *loc8-1* allele does not complement a *prp19* allele. For *loc9*, we crossed SBY482 to SBY382 containing *ESP1-HA3:URA3* and found that the *loc9* ts phenotype segregated away from the *URA3* marker in 20 tetrads.

Plasmid constructions: To determine the minimal complementing region of the genomic clones that suppressed each mutant, we tested previously described plasmids or constructed subclones of the genomic plasmids. For *loc1*, a *CSE4-HA* subclone previously described (STOLER *et al.* 1995) complemented the ts phenotype. The *loc2* data was previously described (BIGGINS *et al.* 1999). For *loc3*, genomic clone pSB333 was digested with *Nar*I and *Nhe*I and the 1020-bp fragment was ligated into pRS316 that was digested with *Clal* and *Spe*I. The resulting clone containing *SMT3*, pSB150, complemented the *loc3* mutant phenotype. A clone containing *pGAL-SMT3* (pSB231) as the sole source of yeast DNA also complemented *loc3* mutant cells. For *loc4*, plasmid pTW004 containing the *CDC7* complemented the ts phenotype. For *loc5*, the genomic clone pNB4 was digested with *Sph*I to eliminate 2 kb of genomic DNA and the backbone vector containing the *PRP16* gene was ligated to create pNB13, which complements the *loc5* mutation. To determine that *PRP16* was the complementing gene on this plasmid, pNB13 was digested with *Xba*I and filled in with the Klenow fragment of DNA polymerase to create pNB20 that contains a frame-shift mutation in the *PRP16* gene. This clone did not complement *loc5*. For *loc6*, a *PDS1* clone, pAY53 (gift of V. Guacci, Fox Chase Cancer Center), complemented the ts phenotype. For *loc7*, DNA encoding just the *YSC4* gene was PCR amplified using primers LOC7-1 (5'-GCG/CGC/GGAT/CCC/GCG/TTG/TTT/TCT/TGT/CG-3') and LOC7-2 (5'-GCG/CGC/GGC/CGC/GGG/TAA/ACG/TCA/GTT/CGA-3') that had *Bam*HI and *Not*I sites engineered, respectively. The PCR product was digested with *Bam*HI and *Not*I and ligated into pRS316 to create pNB27, which complemented the *loc7* ts phenotype. For *loc8*, the *Afl*III site in genomic clone pSB190 was filled in with the Klenow fragment of DNA polymerase to create a frame-shift mutation in the *PRP19* gene. This clone did not complement *loc8*.

We constructed clones to conduct linkage tests. To confirm *PRP19* linkage to the *loc8* mutation, pSB194 was constructed by PCR amplifying the *UBI4* gene from pSB190 using primers SB15 (5'-TCG/ATC/GGA/TCC/GAG/GGC/GGT/TCC/TCC-3') and SB16 (5'-GAT/CGA/TCT/AGA/GAA/AAT/ATT/GCC/AGG/ACT/G-3') that had *Bam*HI and *Xba*I sites engineered, respectively. The PCR product was digested with *Bam*HI and *Xba*I and ligated into pRS306 digested with the same enzymes. The clone was digested with *Bgl*II for integration into yeast.

The intronless tubulin clone, pSB273, was constructed by digesting pRS415/ITUB (gift of John Wagner and Jon Abelson) with *Bam*HI and *Spe*I and the 2.3-kb fragment containing

intronless *TUB1* was ligated into pRS305 digested with *Bam*HI and *Spe*I. The *pGAL-Δ176-CLB2* plasmid, pSB102, was constructed by digesting pAR39 (gift of Adam Rudner) with *Stu*I and ligating this to the 5-kb *Pvu*II fragment isolated from pRS317. The high-copy *smt3-331* suppressor subclone encoding *WSS1* was constructed by PCR amplification of *WSS1* from genomic clone pSB227, using primers SB97 (5'-GAT/CGA/TCG/GAT/CCG/CGG/GCT/TAG/TCA/GCG-3') and SB98 (5'-GAT/CGA/TCG/AAT/TCC/GAG/TTC/TTC/GCT/GTG/G-3') that had *Bam*HI and *Eco*RI sites engineered, respectively. The PCR product was digested with *Bam*HI and *Eco*RI and ligated into pRS426 digested with *Bam*HI and *Eco*RI to create plasmid pSB253. The repressible *CSE4* clone, pSB233, was constructed by PCR amplification of *CSE4* using primers SB82 (5'-GAT/CGA/TCT/GCA/GGA/TGT/CAA/GTA/AAC/AAC/AAT/GG-3') and SB83 (5'-GAT/CGA/TCG/CGG/CCG/CCT/AAA/TAA/ACT/GTC/CCC/TG-3') that had *Pst*I and *Not*I sites, respectively, engineered. The PCR product was digested with *Pst*I and *Not*I and ligated into pNB32 (N. BHALLA, S. BIGGINS and A. W. MURRAY, unpublished results) that was digested with *Pst*I and *Not*I to create pSB233 containing seven tetracycline operators upstream of the *CSE4* gene.

DNA flow cytometry: Approximately 10^7 cells were harvested before and after a 4-hr temperature shift to 37° and fixed in 70% ethanol. Cells were prepared for flow cytometry as described (BISHOP *et al.* 2000) and 20,000 cells from each sample were scanned with a FACScan machine (Becton Dickinson, Franklin Lakes, NJ).

Microscopy: Microscopy to analyze sister chromatids was performed as described (BIGGINS *et al.* 1999). Indirect immunofluorescence was carried out as described (ROSE *et al.* 1990). 4',6-diamidino-2-phenylindole (DAPI) was obtained from Molecular Probes (Eugene, OR) and used at 1 μg/ml final concentration. Chromosome spreads were performed as described (LOIDL *et al.* 1991; MICHAELIS *et al.* 1997). LipsoL was obtained from Lip Ltd. (Shiple, England). 12CA5 antibodies that recognize the hemagglutinin (HA) tag and 9E10 antibodies that recognize the myc tag were used at a 1:1000 dilution and obtained from Covance. Anti-tubulin antibodies yol 1/34 were obtained from Accurate Chemical and Scientific Corp. (Westbury, NY) and used at a 1:1000 dilution. Cy3 secondary antibodies were obtained from Jackson Immunoresearch (West Grove, PA) and used at a 1:2000 dilution. FITC secondary antibodies were obtained from Jackson Immunoresearch and used at a 1:500 dilution.

RESULTS

Isolation of *loc* mutants: We performed microscopy on a bank of temperature-sensitive yeast mutants with a GFP-marked chromosome to isolate mutants defective in chromosome behavior. A tandem repeat of lactose operators (*lacO*) was integrated at the *TRP1* locus, 12 kb from the centromere of chromosome IV, the largest chromosome. A GFP fusion to the lactose repressor (GFP-*lacI*) was expressed in these cells to allow visualization of chromosome IV. We generated a ts bank of conditional yeast mutants in this strain by mutagenizing cells with EMS or UV and screening for lack of growth at 37°. We isolated ~2000 ts mutants that were subsequently screened for chromosome behavior defects using fluorescence microscopy.

The visual screen was conducted by examining large-

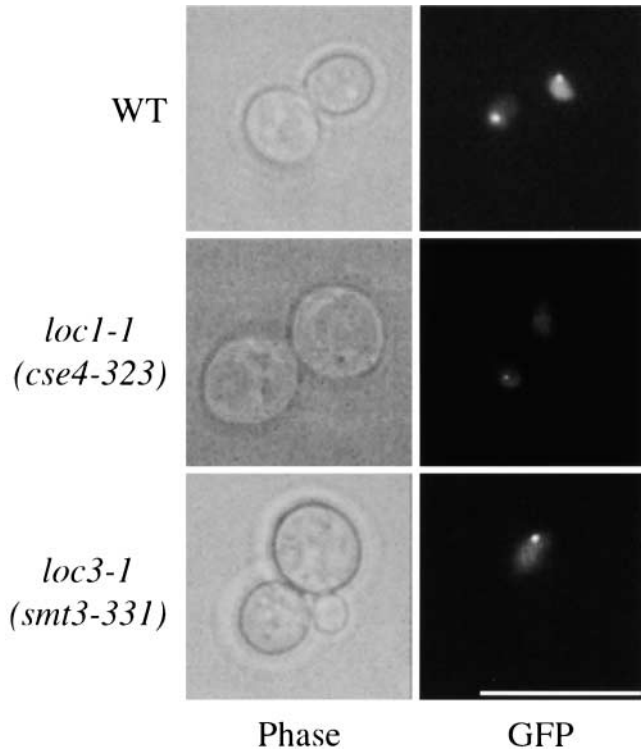


FIGURE 1.—Examples of *loc* mutant sister chromatid phenotypes. Wild-type (SBY214), *loc1-1* (SBY323, *cse4-323*), and *loc3-1* (SBY331, *smt3-331*) strains were shifted to the nonpermissive temperature (37°) for 4 hr and fixed for microscopy. Left, Phase contrast microscopy; right, GFP fluorescence. Wild-type cells separate sister chromatids to opposite poles so there is a GFP signal in each bud. In *loc1-1* cells, there is only one GFP signal in the large-budded cell. In *loc3-1* cells, there is only one GFP signal even though the large-budded cell is rebudding. Bar, 10 μ m.

budded cells. The majority of wild-type cells completed anaphase, resulting in sister chromatids that separated to opposite poles so that two GFP signals are visualized by microscopy (Figure 1). To isolate mutants that are defective in the loss of cohesion at anaphase, we screened ts mutant strains for large-budded cells that contain one GFP signal instead of two signals (see Figure 1 for examples of mutants). Each ts mutant strain was shifted to the nonpermissive temperature (37°) for 4 hr and then screened by fluorescence microscopy for the number of GFP signals in large-budded cells. In this primary screen, we isolated 283 mutant strains from a total of 2000 ts mutant strains, where 50% or more of the large budded cells contained one GFP signal compared to 8% of wild-type large-budded cells.

A variety of defects in addition to sister chromatid separation defects will result in large-budded cells containing one GFP signal. The largest class of mutants will be those that arrest in metaphase instead of proceeding into anaphase, such as mutants that activate the spindle assembly checkpoint and/or the DNA damage or synthesis checkpoints and mutants that are defective in the

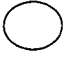



anaphase promoting complex. We therefore performed a number of secondary screens designed to eliminate mutants where a single GFP dot was due to a metaphase delay or arrest.

First, we analyzed sister chromatid separation in an anaphase arrest where wild-type cells separate sister chromatids. The ubiquitin-mediated proteolysis of the major mitotic budding yeast cyclin, Clb2p, is required for cells to exit from anaphase but not for cells to separate sister chromatids. We therefore overexpressed a nondegradable version of Clb2p in each mutant in an attempt to obtain a population of cells enriched in anaphase. Although the overexpression of nondegradable Clb2 will not drive metaphase-arrested cells into anaphase, we reasoned that it might increase the fraction of sister separation in cells that delay in metaphase. Cells were shifted to the nonpermissive temperature for 4 hr in the presence of galactose to induce the expression of nondegradable Clb2p and subsequently screened for sister chromatid separation by microscopy. We eliminated 231 of the 283 potential mutants because they exhibited 50% or greater sister chromatid separation in this test.

Since we could not determine whether cells containing one GFP signal were in metaphase or had proceeded to anaphase, we next eliminated mutants that showed a *cdc* phenotype in which >70% of the population arrested as large-budded cells. Our logic was that strains that exhibited a *cdc* phenotype with unseparated sister chromatids were likely arrested in metaphase due to activation of a checkpoint or a defect in ubiquitin-mediated proteolysis. Although these cells do not separate sister chromatids, this is a secondary consequence of the metaphase arrest and does not necessarily identify genes specifically involved in sister chromatid separation. We therefore analyzed the morphological distribution of the remaining 52 mutant strains after shifting them to the nonpermissive temperature (37°) for 4 hr and eliminated eight mutant strains in which 70% or more of the population contained large-budded cells.

We performed additional secondary tests to enrich for mutants defective in the loss of cohesion rather than other mitotic defects. Although topoisomeraseII (*top2*) mutant cells do not separate sister chromatids, the spindle elongates and attempts to pull the sister chromatids apart. The force of the mitotic spindle leads to chromosome breakage and cell death. We therefore expected that mutants defective in sister chromatid separation would rapidly lose viability as they pass through mitosis at the nonpermissive temperature. To test the mutants for rapid death, they were shifted to the nonpermissive temperature (37°) and plated to the permissive temperature (23°) 0, 2, and 4 hr later to measure viability. Mutants whose viability decreased by at least 50% were retained as *loc* mutants. We reasoned that preventing the lethal anaphase event might rescue the rapid death of the mutants, so we repeated the rapid death experi-

TABLE 2
Cell cycle distribution of *loc* mutants

Mutant	Allele					% sister separation defect ^a
		% unbudded	% small budded	% large budded	% rebudded	
WT	(SBY214)	40	26	32	2	8
<i>loc1-1</i>	<i>cse4-323</i> (SBY323)	27	8	37	28	62
<i>loc1-2</i>	<i>cse4-327</i> (SBY327)	19	5	43	33	46
<i>loc2-1</i>	<i>ipl1-182</i> (SBY713)	50	19	27	4	44
<i>loc2-2</i>	<i>ipl1-321</i> (SBY322)	53	14	26	7	53
<i>loc3-1</i>	<i>smt3-331</i> (SBY331)	30	14	52	3	72
<i>loc4-1</i>	<i>cdc7-355</i> (SBY355)	11	11	66	12	83
<i>loc5-1</i>	<i>prp16-186</i> (SBY712)	36	27	34	4	86
<i>loc6-1</i>	<i>pds1-176</i> (SBY830)	47	18	33	2	39
<i>loc7-1</i>	<i>ycs4-1</i> (NBY290)	29	22	45	4	82
<i>loc8-1</i>	<i>prp19-153</i> (SBY153)	26	26	45	2	78
<i>loc9-1</i>	<i>esp1-478</i> (SBY478)	47	13	24	16	55
<i>top2</i>	<i>top2-4</i> (SBY530)	49	8	37	6	72

^a Percentage of large-budded cells containing one GFP sister chromatid signal instead of two signals.

ment in the presence of nocodazole/benomyl, which causes cells to arrest in prometaphase due to activation of the spindle assembly checkpoint. Mutants were shifted to the nonpermissive temperature in the presence of nocodazole/benomyl and plated for viability 0, 2, and 4 hr later. Eleven mutants whose decline in viability was fully or partly suppressed by depolymerizing the spindle were retained.

The remaining 11 *loc* mutant strains fit our original criteria for mutants defective in the loss of cohesion. We tested whether the mutants were recessive or dominant by crossing each to a wild-type strain and testing each resulting diploid for temperature sensitivity. All of the mutants were recessive. They were then backcrossed once to a wild-type parent strain to generate *MAT α* and *MAT α* strains for complementation testing. Each *loc* mutant strain was crossed to all of the other mutants as well as the *esp1-1* and *top2-4* mutants and tested for growth at the nonpermissive temperature. Complementation testing determined that there were eight unique *LOC* complementation groups and an allele of the *ESPI* gene (Table 2). We isolated two alleles of the *LOC1* and *LOC2* complementation groups and single alleles of the other complementation groups.

We backcrossed each *loc* mutant five times and then retested the mutants for sister chromatid separation after 4 hr at the nonpermissive temperature (37°). All of the mutants had a defect where only one GFP signal was observed in 39% or greater of the large-budded cells (Table 2). We observed that two mutants, *loc1* and *loc2*, had a very similar phenotype in which there was a clear segregation of the bulk of the DNA but pairs of sister chromatids traveled to one pole (for example, see *loc1-1* in Figure 1). The other mutants did not show as much segregation of the bulk of DNA (for example, see *loc3-1* in Figure 1). We next analyzed the cell cycle distribution at the nonpermissive temperature to confirm that the mutants were not arresting as large-budded cells. Mutant strains were shifted to the nonpermissive temperature for 4 hr and the budding index was determined by microscopy. None of the mutants exhibited a classical *cdc* phenotype of >70% large-budded cells, although *loc3-1* and *loc4-1* were enriched for large-budded cells (Table 2).

We next examined DNA content in the *loc* mutants to ensure that the phenotype was not due to a lack of DNA replication or a metaphase arrest. Mutant cells were shifted to the nonpermissive temperature for 4 hr

and then analyzed by flow cytometry analysis for DNA content before and after the temperature shift (Figure 2). Wild-type and *loc5-1* mutant cells showed no significant change in DNA content after the shift to 37°. The *loc4-1* mutant was defective in DNA replication, consistent with the enrichment of large-budded yeast cells reported in Table 2. The *loc3-1* and *loc8-1* mutants exhibited an enrichment of cells with a G2 DNA content. The remaining mutants exhibited very heterogeneous FACS profiles that included cells with increased and decreased ploidy, indications of severe defects in chromosome segregation.

Identification of the genes encoding the *loc* mutants:

To continue characterization of the *loc* mutants, we cloned them by complementation of the ts phenotype using a centromere-based genomic library. Genomic clones were subcloned to isolate the minimal complementing region of DNA. We subsequently confirmed the identity of the genes by linkage analysis and determined that we had isolated mutations in the *CSE4* (*LOC1*), *IPL1* (*LOC2*), *SMT3* (*LOC3*), *CDC7* (*LOC4*), *PRP16* (*LOC5*), *PDS1* (*LOC6*), *YCS4* (*LOC7*), and *PRP19* (*LOC8*) genes in addition to the *ESP1* (*LOC9*) gene (Table 2). These genes are involved in a variety of processes. We previously described that the *ipl1-321* mutants we isolated in the screen have defective kinetochores (BIGGINS *et al.* 1999). The *CSE4* and *SMT3* genes are also implicated in kinetochore function in budding yeast (BROWN *et al.* 1993; MELUH and KOSHLAND 1995; STOLER *et al.* 1995). We found that the *cse4-323* and *cse4-327* alleles we isolated in this screen were different than previously reported *cse4* alleles that exhibit a metaphase arrest with unsegregated DNA (STOLER *et al.* 1995). Instead, the *cse4* alleles we isolated are more similar to *ipl1* mutants that segregate pairs of sister chromatids to a single pole (BIGGINS *et al.* 1999). The *PDS1* and *ESP1* genes are required for sister chromatid separation (CIOSK *et al.* 1998) and the *YCS4* gene is a component of the condensin complex that is required for chromosome condensation (FREEMAN *et al.* 2000). The *PRP16* and *PRP19* mutants are required for RNA splicing (BURGESS *et al.* 1990; CHENG *et al.* 1993). The *CDC7* gene is required for the initiation of DNA replication (HOLLINGSWORTH and SCLAFANI 1990), consistent with our FACS analysis on the *loc4-1* allele that showed a defect in DNA replication. Since the function of *Cdc7* has been extensively studied, we did not characterize the *loc4* mutant further.

Analysis of sister chromatid separation in *loc* mutants:

Since the *LOC* genes are implicated in a variety of processes, we next determined whether the *loc* mutants we isolated are truly defective in sister chromatid separation. We previously found that the small size of the yeast nucleus relative to the resolution limit of light microscopy does not allow us to distinguish whether a single GFP spot is due to a pair of sister chromatids that are still linked or sister chromatids that are separated

but in such close proximity that they cannot be resolved. We therefore used a test that we previously used to determine that *ipl1-321* mutants do not have defects in sister chromatid separation (BIGGINS *et al.* 1999). We analyzed sister chromatid separation in the absence of a spindle, a condition in which separated sisters slowly diffuse apart. Since the absence of a spindle activates the spindle checkpoint, thus inhibiting sister chromatid separation, we did this analysis in a checkpoint mutant.

We constructed double mutants containing *loc* mutations and *mad2Δ*, which destroys the spindle checkpoint. The double mutant strains were arrested in G1 with α -factor and then released into nocodazole/benomyl at the nonpermissive temperature (37°). One hour after the release α -factor was added back to prevent the cells from entering the next cell cycle. We analyzed sister chromatid separation 3 hr after release from G1 (Figure 3). Although the spindle checkpoint keeps wild-type cells from separating their sister chromatids, ~60% of the *mad2Δ* cells contain two visible GFP dots. Since there is no spindle to pull the sister chromatids away from each other, sister chromatid separation never reaches 100% in *mad2Δ* cells that lack a spindle. Like wild-type cells, all of the *loc* mutant strains maintain sister chromatid linkage in the presence of the spindle checkpoint (Figure 3, solid bars). When we analyzed sister chromatid separation in *loc mad2Δ* double mutant strains (Figure 3, open bars), we found that the mutants fell into two classes. The *esp1-478*, *ycs4-1*, *pds1-176*, and *prp19-153* mutant strains failed to fully separate their sister chromatids even in the absence of the spindle checkpoint. The *prp16-186*, *smt3-331*, and *cse4Δ* mutations all allow sisters to separate when the checkpoint is inactivated. We conclude that four of the *LOC* genes are required for the separation of sister chromatids while the others are required to satisfy the spindle checkpoint or to segregate the separated sisters to opposite spindle poles.

Consistent with our data, the *Esp1* and *Pds1* proteins have roles in sister chromatid separation (CIOSK *et al.* 1998). The role of *Ycs4p* in sister chromatid separation will be described elsewhere (N. BHALLA, S. BIGGINS and A. W. MURRAY, unpublished results). We therefore wanted to test whether the remaining protein, *Prp19p*, is also directly involved in sister chromatid separation. Since *PRP19* is involved in DNA repair (SCHMIDT *et al.* 1999), it seemed possible that the *prp19-153 mad2Δ* double mutant did not separate sister chromatids due to activation of the DNA damage checkpoint. We therefore examined sister chromatid separation in a *prp19-153 mad2Δ* strain that was also deleted for the *RAD9* gene, which is essential for the DNA damage checkpoint (Figure 3B). We arrested cells in G1, released them into nocodazole plus benomyl at the nonpermissive temperature, and analyzed sister chromatid separation after 3 hr. As expected, wild-type, *rad9Δ*, and *prp19-153* control strains do not separate sister chromatids. Although

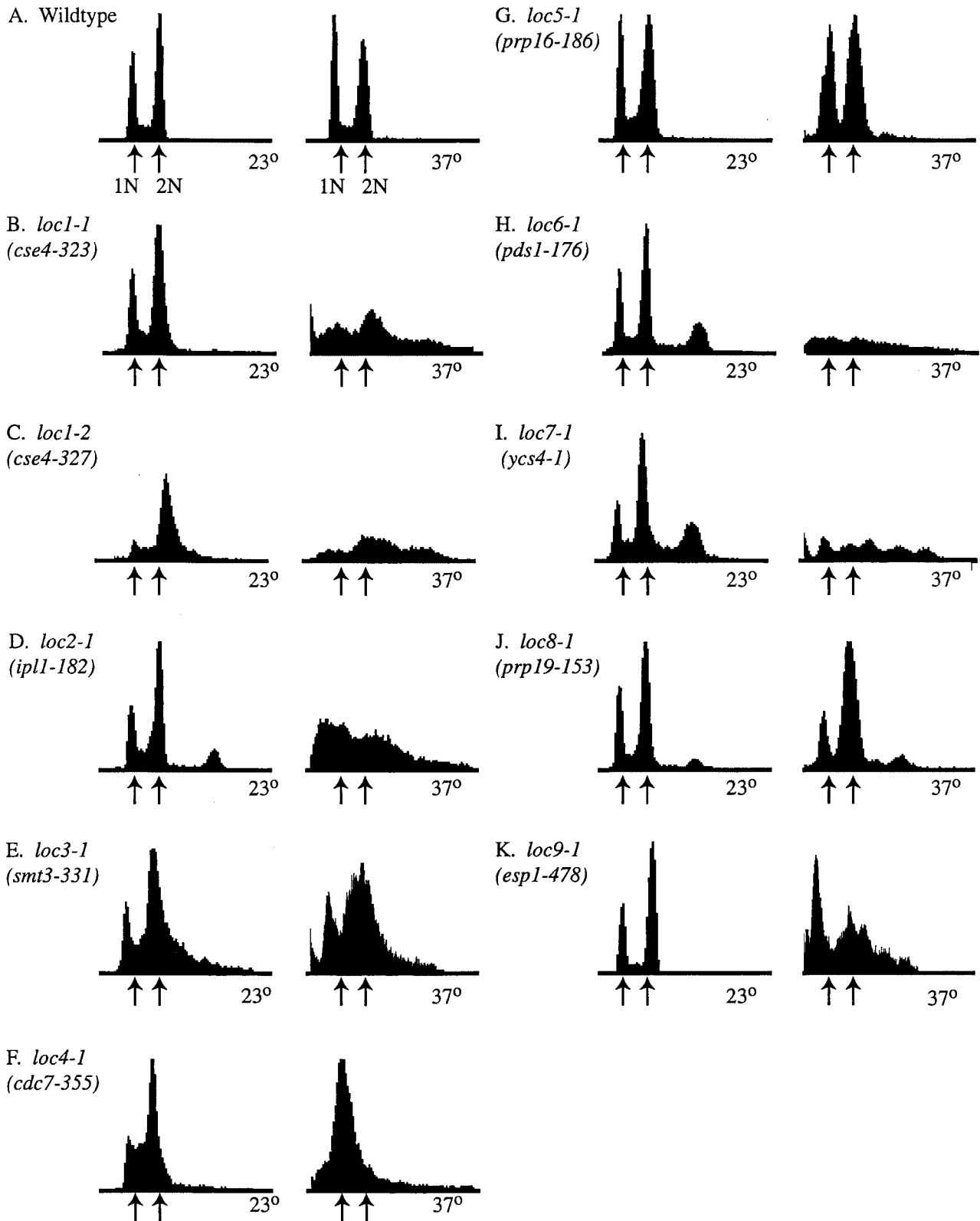
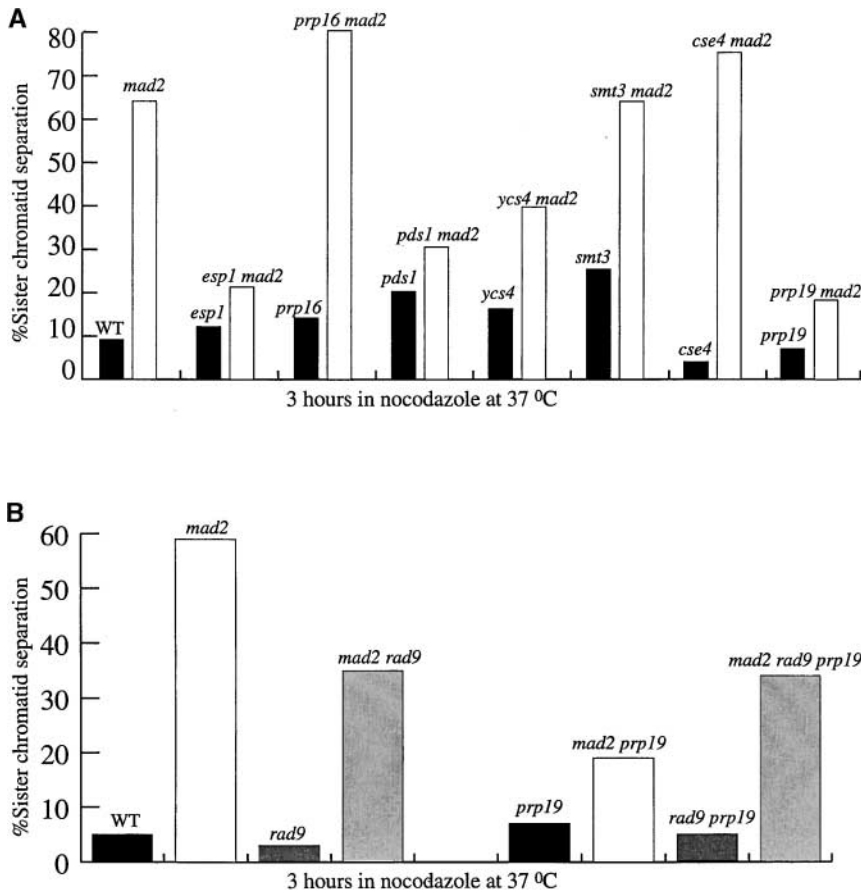


FIGURE 2.—DNA content of *loc* mutant strains. Flow cytometry analysis was performed on *loc* mutant strains at the permissive temperature (23°) and after incubation for 4 hr at the nonpermissive temperature (37°) as indicated. The arrows indicate the 1N (G1) and 2N (G2/M) DNA content. Wild-type [(A) SBY214] and *loc5* mutant cells [(G) SBY712, *prp16-186*] do not show altered DNA content while the *loc1* [(B) SBY323, *cse4-323* and (C) SBY329, *cse4-327*], *loc2* [(D) SBY713, *ipl1-182*], *loc3* [(E) SBY331, *smt3-331*], *loc6* [(H) SBY710, *pds1-176*], *loc7* [(I) SBY828, *ycs4-1*], *loc8* [(J) SBY153, *prp19-153*] and *loc9* [(K) SBY478, *esp1-478*] mutant cells exhibit heterogeneous profiles indicative of chromosome segregation defects. The *loc4* [(F) SBY355, *cdc7-355*] mutant arrests with unreplicated DNA. The FACS profile for *loc2-2* is similar to *loc2-1* and therefore is not shown.



*mad2*Δ (SBY740), and *prp19-153 rad9*Δ (SBY571) cells do not separate sister chromatids. A *mad2*Δ *rad9*Δ *prp19-153* strain (SBY840) separated sister chromatids similar to *mad2*Δ *rad9*Δ cells, indicating that *prp19-153* mutant cells activate the DNA damage checkpoint.

*mad2*Δ cells separate their sisters, we found that a *mad2*Δ *rad9*Δ control strain does not separate sister chromatids to the same levels as a *mad2*Δ strain. This may be due to a slower cell cycle in the *mad2*Δ *rad9*Δ strain (data not shown). Strains containing *prp19-15* and *prp19-153 rad9*Δ mutations do not separate sister chromatids. A *prp19-153 mad2*Δ strain showed an increase in sister chromatid separation relative to the *prp19-153* strain, although it did not reach the levels of the *mad2*Δ control strain, indicating that there are additional mechanisms preventing sister chromatid separation in the *prp19-153* mutant strain. A *prp19-153 mad2*Δ *rad9*Δ triple mutant strain separated sister chromatids to levels similar to the *mad2*Δ *rad9*Δ control strain, suggesting that the *prp19-153* mutant does not have direct defects in sister separation and instead prevents sister separation by activating the DNA damage checkpoint. However, since the levels of sister separation were lower in the *mad2*Δ *rad9*Δ control strain than the *mad2*Δ strain, there may be additional mechanisms controlling sister separation in the *prp19-153* mutant that cannot be detected using this experimental test.

Analysis of spindle function in *loc* mutants: We previously determined that *ipl1-321* mutants have defective

kinetochores, which lead to the *loc* mutant phenotype (BIGGINS *et al.* 1999). Pairs of sister chromatids are often segregated to the same pole, leading to a single GFP dot at one pole instead of a pair of dots at opposite poles. It therefore seemed possible that the *loc* mutants that did not affect sister chromatid separation might have defective kinetochores and/or spindles, which would lead to spindle abnormalities. We therefore analyzed spindle length and morphology in *loc* mutants arrested at metaphase. We constructed double mutants between the *loc* mutant strains and the *cdc23-1* mutant strain that arrests cells in metaphase due to a defect in the ubiquitin-mediated proteolysis of Pds1p. Cells were shifted to the nonpermissive temperature for 4 hr and then analyzed by indirect immunofluorescence for spindle length. The mutants fell into three classes. The first class consists of the *smt3-331 cdc23-1* and *ycs4-1 cdc23-1* double mutant strains that have an average spindle length of 4 μm that is similar to *cdc23-1* single mutant strains (data not shown). In addition, the spindle morphology is indistinguishable from *cdc23-1* single mutant strains. The second class of mutants, consisting of the *pds1-176 cdc23-1* and *cse4-327 cdc23-1* double mutant strains, contained a fraction of cells with spindles that

Figure 3.—Analysis of sister separation in *loc* mutants. (A) Comparison of sister chromatid separation between *loc* (solid bars) and *loc mad2*Δ (open bars) strains. The number of GFP dots was analyzed 3 hr after cells were released from G1 into nocodazole/benomyl-containing medium at the nonpermissive temperature (37°C). After 1 hr at the nonpermissive temperature, α-factor was added to prevent cells from entering the next cell cycle. Wild-type (SBY214), *esp1-478* (SBY468), *prp16-186* (SBY712), *pds1-176* (SBY710), *ycs4-1* (SBY828), *smt3-331* (SBY331), *cse4*Δ (SBY601), and *prp19-153* (SBY153) cells arrest in metaphase with sister chromatids held together (solid bars). When *mad2* was deleted from these cells, sister chromatids separated in *prp16-186* (SBY833), *smt3-331* (SBY567), *cse4*Δ (SBY626), and *mad2*Δ (SBY468) cells and did not fully separate in *esp1-478* (SBY458), *ycs4* (SBY805), *pds1-176* (SBY804), and *prp19-153* (SBY840) mutant cells (open bars). (B) *prp19-153* cells activate the DNA damage checkpoint at the nonpermissive temperature. Sister chromatid separation was analyzed in wild-type (SBY214), *mad2*Δ (SBY468), *rad9*Δ (SBY572), and *mad2 rad9*Δ (SBY849) mutant cells 3 hr after release from G1 into nocodazole/benomyl media at the nonpermissive temperature and revealed that *rad9*Δ mutants delay sister separation in *mad2*Δ mutant cells. *prp19-153* (SBY153), *prp19-153*

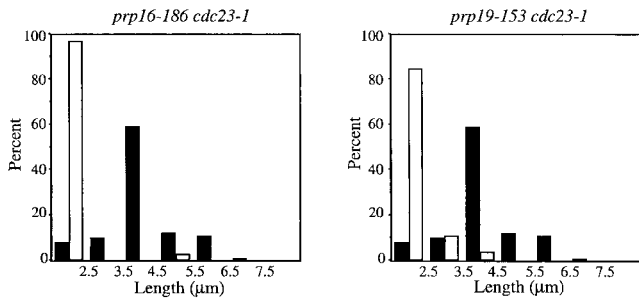


FIGURE 4.—Analysis of spindle length and morphology in *prp16-186* and *prp19-153* mutant strains arrested at metaphase. Indirect immunofluorescence was performed on *cdc23-1 prp* double mutants using anti-tubulin antibodies on cells shifted to the nonpermissive temperature (37°) for 4 hr and spindle length was measured in 200 cells. The percentage of cells at various spindle lengths (μm) is plotted. *prp16-186 cdc23-1* (SBY837) and *prp19-153 cdc23-1* (SBY473) double mutant strains (open bars) had either extremely short or a complete lack of spindles relative to *cdc23-1* mutant strains (SBY186, solid bars).

were shorter than the *cdc23-1* single mutant. While 18% of the *cdc23-1* mutant cells contained spindles shorter than $3.5 \mu\text{m}$, 35% of the *cse4-323 cdc23-1* and *cse4-327 cdc23-1* mutant cells and 47% of the *pds1-176 cdc23-1* mutant cells contained spindles shorter than $3.5 \mu\text{m}$ (data not shown). In addition, 18% of the *pds1-176 cdc23-1* mutant cells contained spindles longer than $5.5 \mu\text{m}$ compared to 12% of the *cdc23-1* mutant cells. These data are consistent with spindle and/or kinetochore defects in these strains. The third class, *prp16-186 cdc23-1* and *prp19-153 cdc23-1*, contained a majority of cells with either extremely short or undetectable spindles (Figure 4). We did not test the *esp1-478* mutant since *ESPI* has known roles in both sister chromatid separation and spindle function (Ciosk *et al.* 1998; Uhlmann *et al.* 2000; Jensen *et al.* 2001).

Since the mutants in the third class are both involved in splicing, we considered the possibility that the phenotype was a consequence of a defect in the splicing of one or more transcripts. One likely candidate is the major α -tubulin gene, *TUB1*, which encodes one of the subunits of the tubulin dimer that polymerizes to form microtubules. Imbalances between the expression of α - and β -tubulin lead to defects in microtubule polymerization and spindle assembly. To test this possibility, we integrated a copy of *TUB1* that did not contain an intron into the *prp16-186 cdc23-1* and *prp19-153 cdc23-1* double mutant strains. We shifted cells to the nonpermissive temperature for 4 hr and then performed indirect immunofluorescence to analyze spindles in the mutant strains with and without intronless tubulin (Figure 5). Although there was little or no tubulin polymer in the *cdc23 prp* mutant strains containing only wild-type *TUB1*, the addition of the intronless tubulin gene restored microtubules and completely suppressed the spindle defect in these strains. Since intronless tubulin sup-

pressed the lack of spindles in the *prp cdc23* double mutants, we tested whether it suppressed the growth defects of these strains. When cells were struck onto plates at 23° , 30° , or 37° there was no difference between the growth of strains with intron-containing or intronless *TUB1* (data not shown), which is consistent with the presence of additional essential transcripts that need to be spliced for viability.

Analysis of *smt3-331* phenotypes: We continued to characterize the *smt3-331* mutant to learn more about the role of Smt3p in chromosome behavior. We first analyzed sister chromatid separation throughout the cell cycle. Wild-type and *smt3-331* mutant cells containing the GFP-marked chromosome were arrested in G1 with α -factor and then released to the nonpermissive temperature (37°). One hour after the release, we added α -factor back to prevent cells from entering the next cell cycle and analyzed sister chromatid separation by microscopy (Figure 6A). Although there was a delay in sister chromatid separation relative to wild-type cells, $\sim 80\%$ of the cells eventually separated sister chromatids. However, sister chromatid separation was abnormal and the two GFP signals never separated as far apart from each other as the wild-type GFP signals (Figure 6B). When *smt3-331* mutant cells were analyzed at later time points (4 hr after release from G1), there was an accumulation of large-budded cells with a single GFP signal (see Table 2 and Figure 1), consistent with its isolation in the *loc* screen.

The *smt3-331* sister separation phenotype suggested that the spindle might not be elongating in these cells. We therefore performed indirect immunofluorescence microscopy on wild-type and *smt3* mutant cells that were grown at the nonpermissive temperature (37°) for 4 hr to analyze spindles. We used anti-tubulin antibodies to visualize the spindles and DAPI staining to visualize the DNA (Figure 7A). We scored large-budded cells and found that 61% of wild-type cells have completed anaphase and have long spindles and 39% are in metaphase with short spindles. In contrast, only 14% of *smt3* large-budded cells have elongated spindles and the remaining 86% are in metaphase with short spindles. To confirm that the *smt3* mutant cells containing short spindles are in metaphase, we performed indirect immunofluorescence against a metaphase marker protein, Pds1. Wild-type and *smt3* mutants were shifted to the nonpermissive temperature for 4 hr and fixed for microscopy. We analyzed Pds1 using anti-myc antibodies that recognize a Myc-tagged Pds1 protein, anti-tubulin antibodies to visualize the spindle, and DAPI staining to visualize the DNA (data not shown). We found that all wild-type and *smt3* large-budded cells containing short spindles had high levels of Pds1 protein, consistent with them being in metaphase.

To determine whether the metaphase delay in the *smt3-331* mutant was due to activation of the spindle checkpoint, we deleted the *MAD2* checkpoint gene and

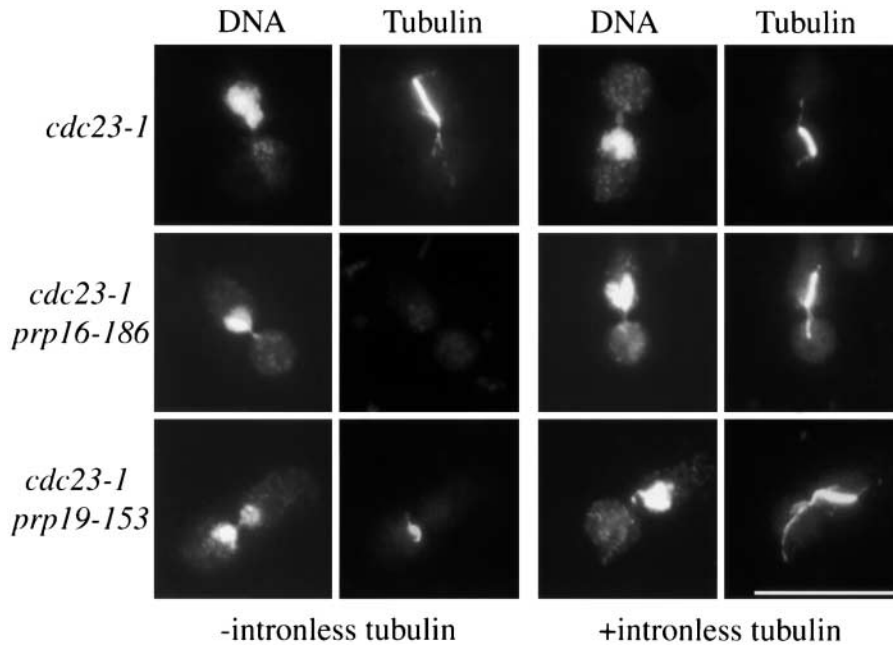


FIGURE 5.—Intronless tubulin alleviates the spindle defect in the *prp* mutants. Indirect immunofluorescence was performed on *cdc23-1* (SBY186), *cdc23-1 prp16-186* (SBY837), and *cdc23-1 prp19-153* (SBY473) mutant strains without intronless tubulin (left) and *cdc23-1* (SBY809), *cdc23-1 prp16-186* (SBY810), and *cdc23-1 prp19-153* (SBY850) mutant strains with intronless tubulin (right). Cells were shifted to the nonpermissive temperature (37°) for 4 hr. DAPI staining is shown on the left and anti-tubulin staining is shown on the right of each part. Bar, 10 μ m.

performed indirect immunofluorescence. We stained cells with DAPI to visualize the DNA and with anti-tubulin antibodies to visualize the spindle and scored the cells for spindle length (Figure 7A). There is no change in the distribution of large-budded cells with short spindles in the *smt3-331* mutant cells *vs.* the *smt3-331 mad2 Δ* mutant cells, suggesting that the *smt3-331* mutant does not activate the spindle checkpoint. To further test this, we analyzed Pds1 protein levels in *smt3-331* and *smt3-331 mad2* mutant cells and determined that Pds1p levels were high in both strains when the spindles were short (data not shown). We also analyzed the percentage of large-budded cells after a temperature shift to 37° and found no change in the number of large-budded cells (data not shown). Therefore, *smt3-331* mutant cells do not accumulate in metaphase due to activation of the spindle checkpoint.

We were surprised that such a high percentage of *smt3* mutant cells were in metaphase since our analysis of sister chromatid separation during a synchronized cell cycle showed that the majority of cells had two GFP signals, consistent with sister chromatid separation. We therefore analyzed sister chromatids by indirect immunofluorescence after 4 hr at the nonpermissive temperature (data not shown). In the cells with short spindles, 68% of the *smt3* mutant cells had one GFP signal and 32% had two GFP signals. In wild-type cells, 79% of the cells with short spindles have a single GFP signal and 21% have two GFP signals. Therefore, *smt3* mutant cells accumulate large-budded cells with short spindles and a single GFP signal when held at the nonpermissive temperature for 4 hr. Therefore, the difference in percentage of sister chromatid separation between the various experiments is unclear and will need to be investigated in the future.

Isolation of *WSSI*, a high-copy *smt3-331* suppressor:

Since the role of *SMT3* in chromosome behavior is unknown, we isolated high-copy suppressors in an effort to identify targets and/or regulators of *SMT3* function. The *smt3-331* mutant strain was transformed with a 2- μ m genomic yeast library and plated onto selective media at the nonpermissive temperature (37°). Suppressing plasmids contained either the *SMT3* gene or a novel gene encoded by yeast open reading frame YHR134W that we named *WSSI* (weak suppressor of *smt3*). High-copy *WSSI* suppresses the *smt3-331* growth defects up to 34.5° but is an extremely weak suppressor at 37° (Figure 7B). In addition, it partially suppresses the cold-sensitive phenotype of the *smt3-331* mutant strain at 14° (data not shown). Since the *smt3-331* mutant strain accumulates large-budded cells, we tested whether high-copy *WSSI* suppresses this phenotype. Wild-type, *smt3-331*, and *smt3-331 2 μ WSSI* cells were shifted to 34.5° or 37° for 4 hr and their morphology was scored. However, we did not detect a significant reduction in the number of large-budded cells in *smt3-331* cells containing high-copy *WSSI* compared to *smt3-331* cells lacking the suppressor (data not shown). We made the *wss1 Δ* mutant to determine if it has phenotypes similar to *smt3-331* mutant cells. There was no obvious growth defect for the *wss1 Δ* strain at 23°, 30°, 33°, 35°, or 37° [data not shown and WINZELER *et al.* (1999)]. However, *wss1 Δ* cells are slightly cold sensitive at 14° (data not shown).

Smt3p localizes to chromosomes: Since *smt3-331* mutant strains have defects in chromosome segregation, we tested whether Smt3p localizes to chromosomes. It was previously reported, using indirect immunofluorescence, that Smt3p localizes to the nucleus and the bud neck (JOHNSON and BLOBEL 1999; TAKAHASHI *et*

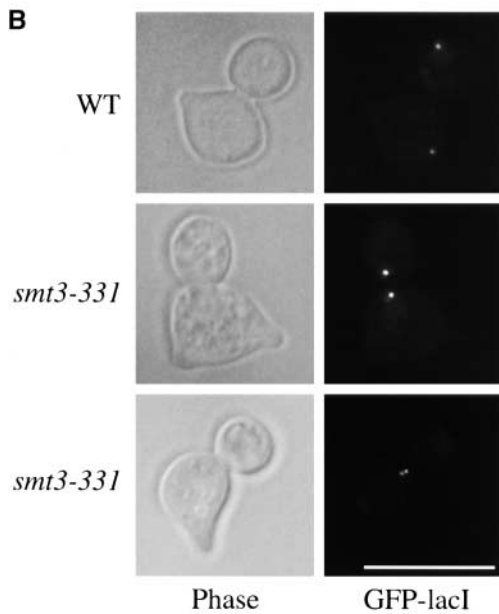
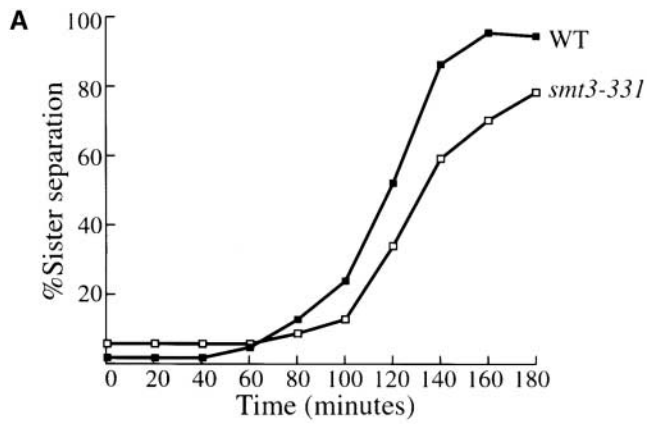


FIGURE 6.—Analysis of sister chromatids in the *smt3-331* mutant. (A) Sister chromatid separation is delayed in *smt3-331* mutant cells. Wild-type (SBY214) and *smt3-331* (SBY333) strains released from α -factor arrest ($T = 0$) to the nonpermissive temperature (37°) were scored for sister chromatid separation. (B) Phenotypes of *smt3-331* mutant cells at $T = 120$ min are shown. (Left) Phase contrast microscopy; (right) fluorescence. Sister chromatids do not separate as far apart in the *smt3-331* mutant cells as they do in wild-type cells. Bar, 10 μ m.

al. 1999). We used chromosome spreads to test whether Smt3p specifically associates with chromosomes. Since Smt3p conjugates to substrates via its C terminus, we epitope tagged Smt3 at the N terminus under the control of the galactose promoter. We performed chromosome spreads on a strain expressing HA3-Smt3p induced by galactose and stained the spreads with anti-HA antibodies to visualize Smt3p and DAPI to visualize the chromosomes (Figure 8). Overexpressed Smt3p stained chromosome spreads brightly using this technique, consistent with its role in chromosome segregation.

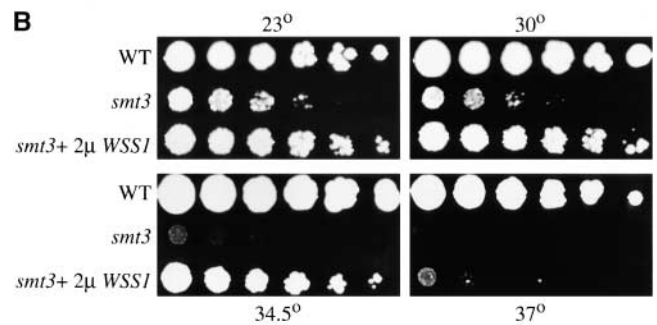
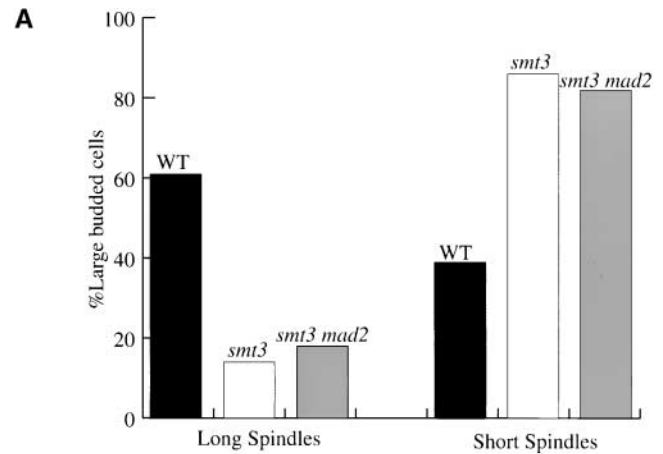


FIGURE 7.—Analysis of *smt3-331* mutant phenotypes and the isolation of a high-copy suppressor. (A) *smt3-331* mutant cells accumulate in metaphase. Wild-type (SBY214, solid bars), *smt3-331* (SBY331, open bars), and *smt3-331 mad2* (SBY567, shaded bars) strains were shifted to 37° for 4 hours and then harvested for indirect immunofluorescence using anti-tubulin antibodies. The percentages of large budded cells with either short spindles (right) or long spindles (left) are plotted and show that *smt3-331* and *smt3-331 mad2* mutant strains are enriched for cells with short spindles. (B) Isolation of WSS1. High-copy WSS1 suppresses the *smt3-331* mutant growth defects. Fivefold serial dilutions of wild-type (SBY214), *smt3-331* (SBY331), and *smt3-331* with 2μ WSS1 (SBY696) cells were plated at 23° , 30° , 34.5° , and 37° . High-copy WSS1 suppresses *smt3-331* growth defects up to 34.5° but is a poor suppressor at 37° .

DISCUSSION

We isolated mutants in nine *LOC* genes by screening temperature-sensitive strains containing a GFP-marked chromosome for defects in sister chromatid separation. By analyzing sister chromatid separation in the mutant strains in the absence of a spindle, we classified the mutants for direct *vs.* indirect effects on sister chromatid separation. We determined that the *esp1-478*, *pds1-176*, and *ycs4-1* mutant strains are defective in sister chromatid separation whereas the *cse4*, *ipl1*, and *smt3-331* mutant strains affect chromosome segregation. The *prp16-186* and *prp19-153* mutant strains are defective in processing the *TUB1* transcript, leading to an apparent *loc* phenotype. We characterized the *smt3-331* mutant

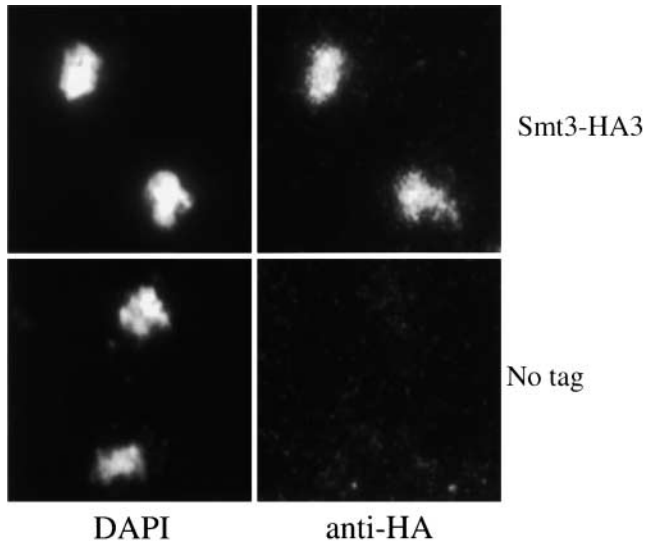


FIGURE 8.—Smt3p localizes to chromosomes. Indirect immunofluorescence of chromosome spreads of a strain expressing pGAL-HA3-Smt3p shows that Smt3p localizes to chromosomes (top, SBY761). There is no staining in a strain that does not contain an epitope-tagged protein (bottom, SBY516). Left, DAPI staining; right, anti-HA staining.

strain and found it has an increased number of cells in metaphase. In addition, we isolated a high-copy suppressor of the *smt3-331* ts phenotype, *WSSI*. Smt3p localizes to chromosomes, consistent with a role in chromosome segregation.

Genes involved in sister chromatid separation and segregation: Although the *LOC* screen was originally designed to isolate mutants specifically defective in sister chromatid separation, secondary tests determined that mutants defective in sister chromatid separation exhibit phenotypes similar to mutants that cause nondisjunction of sister chromatids. We previously found that the *ipl1* alleles isolated in the screen have defective kinetochores that frequently result in both sister chromatids segregating to a single pole. Since both chromosomes are close to the spindle pole they are rarely separated by more than the resolution limit of the light microscope. By depolymerizing the spindle, we allow the sisters to drift apart, making a clear distinction between sister separation and sister segregation mutants. Applying this test revealed that the only three *loc* mutants directly required for sister chromatid separation encode the *ESPI*, *YCS4*, and *PDS1* genes. The Esp1 and Pds1 proteins have previously been shown to be required for sister chromatid separation (Ciosk *et al.* 1998). Additional work from our lab on Ycs4p has also revealed a role in sister chromatid separation (N. BHALLA, S. BIGGINS and A. W. MURRAY, unpublished results). *PDS1* appears to have dual roles in regulating sister chromatid separation. Although Pds1p inhibits the activation of the Esp1 protein, a complete deletion of the *PDS1* gene does not lead to precocious sister chromatid separation (Ciosk *et al.* 1998). Instead, *pds1Δ* strains are delayed

in sister chromatid separation, indicating that Pds1 has a positive role in promoting separation in addition to a negative role inhibiting Esp1p. However, if *pds1Δ* strains are held in nocodazole for extended periods of time, they eventually separate sister chromatids due to defects in inhibiting Esp1p activity (GUACCI *et al.* 1997). Elimination of the fission yeast Pds1 homolog, Cut2, completely prevents sister separation (FUNABIKI *et al.* 1996). The *pds1-176* allele we isolated is phenotypically more similar to the phenotype of *cut2Δ* cells in fission yeast. We do not know if the difference between our results and previous experiments on *pds1Δ* strains reflects a difference in experimental procedures or the ability of our *pds1-176* allele to interfere with the function of Esp1 more severely than the complete absence of Pds1p. The *esp1-478* mutation we isolated behaves like *esp1-1* in the tests in this article. Although our screen was far from saturated, two of the three mutants that affected sister separation identified previously identified genes. This outcome suggests that there may not be many genes directly required for sister separation or that there may be a number of additional genes involved in sister chromatid separation that are not amenable to being mutated to produce temperature-sensitive phenotypes.

We analyzed spindles during a metaphase arrest as a secondary test to determine whether the *loc* mutants that were not directly defective in sister chromatid separation have defects in spindle function or morphology. The *smt3-331* mutant strain did not exhibit any spindle defects in the metaphase arrest, consistent with the isolation of *SMT3* as a suppressor of mutations in *MIF2*, a known kinetochore component (MELUH and KOSHLAND 1995). If Smt3p regulates kinetochores, it must do so in a manner that does not affect kinetochore/microtubule attachments during a metaphase arrest, leading to changes in spindle length or morphology (see below for further discussion). We found that a fraction of *cse4-327* and *pds1-176* mutants exhibit spindle defects in a metaphase arrest. Since Cse4p is localized to kinetochores and *cse4* mutant strains have defects in kinetochore function, it is likely that *cse4-327* mutants exhibit defects due to defective kinetochores. It was previously found that *pds1* mutant strains elongate spindles in a metaphase arrest due to lack of cohesion between sister chromatids. Our allele also behaves differently in this test. We found a large distribution in spindle length in the *pds1-176 cdc23-1* mutant strain arrested at metaphase. Although some of the cells elongate spindles, 47% have shorter spindles than cells arrested in metaphase. This suggests that this *pds1-176* allele may affect kinetochore or spindle function in addition to sister chromatid separation, consistent with a recent report showing that Pds1 mediates Esp1p localization to spindles (JENSEN *et al.* 2001).

Genes involved in splicing: We isolated mutations in two genes involved in RNA splicing in the *loc* screen: *PRP16* and *PRP19*. Although both genes are essential

for splicing, the *PRP19* gene is also required for DNA repair (SCHMIDT *et al.* 1999). Since these genes have well-established roles in RNA processing, we reasoned that it was likely we isolated them as a secondary consequence of defects in splicing the transcripts of one or more genes important for chromosome segregation. There are only 270 transcripts in budding yeast that are spliced, and the most obvious candidate for a gene that could lead to a lack of spindles in a metaphase was the major α -tubulin gene, *TUB1*. We found that an intronless version of *TUB1* that did not need to be spliced completely rescued the spindle defect during the metaphase arrest. However, the intronless tubulin did not change the temperature sensitivity of these mutants, consistent with there being other essential intron-containing transcripts, such as the ribosomal protein genes.

Our evidence suggests that the *prp19-153* allele we isolated activates the DNA damage checkpoint. We had to delete both the spindle checkpoint and the DNA damage checkpoint in this mutant to detect sister chromatid separation in the absence of a spindle. This was not true for the *prp16-186* allele, which separated sister chromatids in the absence of a spindle. Therefore, the *prp19-153* mutant has an additional defect. It is likely that this mutant activates the DNA damage checkpoint due to its role in DNA repair.

Analysis of *SMT3* and *WSSI*: We report an initial characterization of phenotypes associated with defects in the *SMT3/SUMO* gene in budding yeast. Although the *smt3-331* mutant strain does not exhibit a cell cycle arrest, there is an enrichment of large-budded cells in metaphase containing short spindles and high levels of Pds1 protein. These cells are not delayed in metaphase due to activation of the spindle checkpoint because deletion of the checkpoint did not change the phenotypes of *smt3-331* mutant strains. Therefore, these mutants may activate another checkpoint or instead regulate the proteolysis of proteins involved in the transition from metaphase to anaphase.

Although the *SMT3* gene was originally identified as a suppressor of a *mif2* kinetochore mutant, the *smt3-331* mutant strain does not exhibit a spindle checkpoint-dependent arrest in metaphase. In addition, the kinetochores must be functional for microtubule binding in *smt3-331* mutant cells since sister chromatids are pulled toward opposite poles. It is therefore likely that the suppression of the *mif2* kinetochore mutant by *SMT3* overexpression is related to a different aspect of kinetochore function. This may include some aspect of cohesin loading or centromeric chromatin structure that could lead to premature separation of the centromere-proximal regions of the chromosomes.

A previous study localized Smt3p to the bud neck and the nucleus by indirect immunofluorescence (JOHNSON and BLOBEL 1999). We used chromosome spreads to more specifically localize Smt3 protein within the nucleus to determine whether the protein binds to chro-

mosomes and/or kinetochores. We found that Smt3 is associated with chromosomes when overexpressed, suggesting a general role in chromosome structure or function. This would also be consistent with the *smt3-331* mutant cells not exhibiting obvious kinetochore defects. Further work localizing the endogenous protein will be required to know the precise localization pattern.

Since the role of Smt3p in chromosome segregation is unknown, we isolated a high-copy suppressor of the temperature sensitivity to identify key regulators/substrates. We isolated one suppressor, called *WSSI*, which is predicted to encode a 30-kD protein of unknown function. It has two homologs in *Schizosaccharomyces pombe*, Spcc1442.07cp and Spac521.02p, which exhibit 47 and 57% similarity and 28 and 39% identity, respectively. Although the Spcc1442.07cp protein is a putative Zinc protease, the Wss1 protein does not have any obvious motifs that would suggest function. We analyzed the sequence for the Smt3p conjugation consensus sequence in the septins (ILV)KX(ED), but did not find this sequence. It is not known whether there are other consensus Smt3p conjugation sites. It is not clear whether Wss1p suppresses the *smt3-331* mutant because it is an Smt3p substrate, Smt3p regulator, or has overlapping functions. *WSSI* is not essential and *wss1 Δ* strains do not exhibit any severe phenotypes except a mild cold sensitivity, making its function less clear. Although we have not tested whether Smt3p directly conjugates to Wss1p, the Wss1-myc13 epitope-tagged protein migrates at a much higher molecular weight than predicted on polyacrylamide gels, which would be consistent with conjugation (data not shown). Future studies will be required to determine the exact nature of the interaction between Wss1p and Smt3p.

Our analysis suggests that the control of mitotic chromosome behavior is complex and that many genes are involved in the process. The alleles of *CSE4* and *PDS1* we isolated appear to behave qualitatively differently than previously identified alleles. More detailed analysis of the alleles we isolated will help to determine the roles of these genes and others (*SMT3* and *YSC4*) in mitotic chromosome behavior.

We are very grateful to past and present members of the Murray and Morgan labs for invaluable help and discussions about this project. We thank the following people for strains and plasmids: John Wagner and John Abelson; the Guthrie and Morgan labs; and Adam Rudner, Aaron Straight, Doug Kellogg, Vinny Guacci, and Joachim Li. We appreciate Aaron Straight's advice and support in working with the GFP system and Jeff Ubersax's help with FACS analysis. We thank Stéphanie Buvelot for critically reading the manuscript. This work was supported by Jane Coffin Childs and American Cancer Society postdoctoral fellowships to S.B., a National Science Foundation predoctoral fellowship to N.B., and grants from the National Institutes of Health and the Human Frontier Science Program to A.W.M.

LITERATURE CITED

- BIGGINS, S., F. F. SEVERIN, N. BHALLA, I. SASSOON, A. A. HYMAN *et al.*, 1999 The conserved protein kinase Ipl1 regulates microtubule

- binding to kinetochores in budding yeast. *Genes Dev.* **13**: 532–544.
- BISHOP, A. C., J. A. UBERSAX, D. T. PETSCH, D. P. MATHEOS, N. S. GRAY *et al.*, 2000 A chemical switch for inhibitor-sensitive alleles of any protein kinase. *Nature* **407**: 395–401.
- BROWN, M. T., L. GOETSCH and L. H. HARTWELL, 1993 MIF2 is required for mitotic spindle integrity during anaphase spindle elongation in *Saccharomyces cerevisiae*. *J. Cell Biol.* **123**: 387–403.
- BURGESS, S., J. R. COUTO and C. GUTHRIE, 1990 A putative ATP binding protein influences the fidelity of branchpoint recognition in yeast splicing. *Cell* **60**: 705–717.
- CHENG, S. C., W. Y. TARN, T. Y. TSAO and J. ABELSON, 1993 *PRP19*: a novel spliceosomal component. *Mol. Cell Biol.* **13**: 1876–1882.
- CIOSK, R., W. ZACHARIAE, C. MICHAELIS, A. SHEVCHENKO, M. MANN *et al.*, 1998 An ESP1/PDS1 complex regulates loss of sister chromatid metaphase to anaphase transition in yeast. *Cell* **93**: 1067–1076.
- CIOSK, R., M. SHIRAYAMA, A. SHEVCHENKO, T. TANAKA, A. TOTH *et al.*, 2000 Cohesin's binding to chromosomes depends on a separate complex consisting of Scc2 and Scc4 proteins. *Mol. Cell* **5**: 243–254.
- COHEN-FIX, O., J. M. PETERS, M. W. KIRSCHNER and D. KOSHLAND, 1996 Anaphase initiation in *Saccharomyces cerevisiae* is controlled by the APC-dependent degradation of the anaphase inhibitor Pds1p. *Genes Dev.* **10**: 3081–3093.
- FRANCISCO, L., W. WANG and C. S. CHAN, 1994 Type 1 protein phosphatase acts in opposition to Ipl1 protein kinase in regulating yeast chromosome segregation. *Mol. Cell Biol.* **14**: 4731–4740.
- FREEMAN, L., L. ARAGON-ALCAIDE and A. STRUNNIKOV, 2000 The condensin complex governs chromosome condensation and mitotic transmission of rDNA. *J. Cell Biol.* **149**: 811–824.
- FUNABIKI, H., H. YAMANO, K. KUMADA, K. NAGAO, T. HUNT *et al.*, 1996 Cut2 proteolysis required for sister-chromatid separation in fission yeast. *Nature* **381**: 438–441.
- GARDNER, R. D., and D. J. BURKE, 2000 The spindle checkpoint: two transitions, two pathways. *Trends Cell Biol.* **10**: 154–158.
- GUACCI, V., D. KOSHLAND and A. STRUNNIKOV, 1997 A direct link between sister chromatid cohesion and chromosome condensation revealed through the analysis of *MCD1* in *S. cerevisiae*. *Cell* **91**: 47–57.
- HARDWICK, K., and A. W. MURRAY, 1995 Mad1p, a phosphoprotein component of the spindle assembly checkpoint in budding yeast. *J. Cell Biol.* **131**: 709–720.
- HARTMAN, T., K. STEAD, D. KOSHLAND and V. GUACCI, 2000 Pds5p is an essential chromosomal protein required for both sister chromatid cohesion and condensation in *Saccharomyces cerevisiae*. *J. Cell Biol.* **151**: 613–626.
- HIRANO, T., 2000 Chromosome cohesion, condensation, and separation. *Annu. Rev. Biochem.* **69**: 115–144.
- HIRANO, T., and T. J. MITCHISON, 1994 A heterodimeric coiled-coil protein required for mitotic chromosome condensation in vitro. *Cell* **79**: 449–458.
- HIRANO, T., R. KOBAYASHI and M. HIRANO, 1997 Condensins, chromosome condensation protein complexes C, XCAP-E and a Xenopus homolog of the Drosophila Barren. *Cell* **89**: 511–521.
- HOLLINGSWORTH, R. E., JR., and R. A. SCLAFANI, 1990 DNA metabolism gene *CDC7* from yeast encodes a serine (threonine) protein kinase. *Proc. Natl. Acad. Sci. USA* **87**: 6272–6276.
- JENSEN, S., M. SEGAL, D. J. CLARKE and S. I. REED, 2001 A novel role of the budding yeast separin *espl1* in anaphase spindle elongation. Evidence that proper spindle association of *espl1* is regulated by *pds1*. *J. Cell Biol.* **152**: 27–40.
- JOHNSON, E. S., and G. BLOBEL, 1999 Cell cycle-regulated attachment of the ubiquitin-related protein SUMO to the yeast septins. *J. Cell Biol.* **147**: 981–994.
- KAPLAN, K. B., A. A. HYMAN and P. K. SORGER, 1997 Regulating the yeast kinetochore by ubiquitin-dependent degradation and Skp1p-mediated phosphorylation. *Cell* **91**: 491–500.
- LAVOIE, B. D., K. M. TUFFO, S. OH, D. KOSHLAND and C. HOLM, 2000 Mitotic chromosome condensation requires Brn1p, the yeast homologue of Barren. *Mol. Biol. Cell* **11**: 1293–1304.
- LECHNER, J., and J. CARBON, 1991 A 240 Kd multisubunit complex, CBF3, is a major component of the budding yeast centromere. *Cell* **64**: 717–725.
- LOIDL, J., K. NAIRZ and F. KLEIN, 1991 Meiotic chromosome synapsis in a haploid yeast. *Chromosoma* **100**: 221–228.
- LONGTINE, M. S., A. MCKENZIE, 3RD, D. J. DEMARINI, N. G. SHAH, A. WACH *et al.*, 1998 Additional modules for versatile and economical PCR-based gene deletion and modification in *Saccharomyces cerevisiae*. *Yeast* **14**: 953–961.
- MAHAJAN, R., C. DELPHIN, T. GUAN, L. GERACE and F. MELCHIOR, 1997 A small ubiquitin-related polypeptide involved in targeting RanGAP1 to nuclear pore complex protein RanBP2. *Cell* **88**: 97–107.
- MATUNIS, M. J., E. COUTAVAS and G. BLOBEL, 1996 A novel ubiquitin-like modification modulates the partitioning of the Ran-GTPase-activating protein RanGAP1 between the cytosol and the nuclear pore complex. *J. Cell Biol.* **135**: 1457–1470.
- MELUH, P. B., and D. KOSHLAND, 1995 Evidence that the *MIF2* gene of *Saccharomyces cerevisiae* encodes a centromere protein with homology to the mammalian centromere protein CENP-C. *Mol. Biol. Cell* **6**: 793–807.
- MELUH, P. B., and D. KOSHLAND, 1997 Budding yeast centromere composition and assembly as revealed by in vivo cross-linking. *Genes Dev.* **11**: 3401–3412.
- MELUH, P. B., P. YANG, L. GLOWCZEWSKI, D. KOSHLAND and M. M. SMITH, 1998 Cse4p is a component of the core centromere of *Saccharomyces cerevisiae*. *Cell* **94**: 607–613.
- MICHAELIS, C., R. CIOSK and K. NASMYTH, 1997 Cohesins: chromosomal proteins that prevent premature separation of sister chromatids. *Cell* **91**: 35–45.
- NASMYTH, K., J. M. PETERS and F. UHLMANN, 2000 Splitting the chromosome: cutting the ties that bind sister chromatids. *Science* **288**: 1379–1385.
- OUSPENSKI, O., II, A. CABELLO and B. R. BRINKLEY, 2000 Chromosome condensation factor Brn1p is required for chromatid separation in mitosis. *Mol. Biol. Cell* **11**: 1305–1313.
- PIDOUX, A. L., and R. C. ALLSHIRE, 2000 Centromeres: getting a grip of chromosomes. *Curr. Opin. Cell Biol.* **12**: 308–319.
- ROSE, M. D., F. WINSTON and P. HEITER, 1990 *Methods in Yeast Genetics*. Cold Spring Harbor Laboratory Press, Cold Spring Harbor, NY.
- SAITOH, H., R. T. PU and M. DASSO, 1997 SUMO-1: wrestling with a new ubiquitin-related modifier. *Trends Biochem. Sci.* **22**: 374–376.
- SCHMIDT, C. L., M. GREY, M. SCHMIDT, M. BRENDDEL and J. A. HENRIQUES, 1999 Allelism of *Saccharomyces cerevisiae* genes *PSO6*, involved in survival after 3-CPs+UVA induced damage, and *ERG3*, encoding the enzyme sterol C-5 desaturase. *Yeast* **15**: 1503–1510.
- SHERMAN, F., G. FINK and C. LAWRENCE, 1974 *Methods in Yeast Genetics*. Cold Spring Harbor Laboratory Press, Cold Spring Harbor, NY.
- SKIBBENS, R. V., L. B. CORSON, D. KOSHLAND and P. HIETER, 1999 Ctf7p is essential for sister chromatid cohesion and links mitotic chromosome structure to the DNA replication machinery. *Genes Dev.* **13**: 307–319.
- SORGER, P. K., K. F. DOHENY, P. HIETER, K. M. KOPSKI, T. C. HUFFAKER *et al.*, 1995 Two genes required for the binding of an essential *Saccharomyces cerevisiae* kinetochore complex to DNA. *Proc. Natl. Acad. Sci. USA* **92**: 12026–12030.
- STEMMANN, O., and J. LECHNER, 1996 The *Saccharomyces cerevisiae* kinetochore contains a cyclin-CDK complexing homologue, as identified by in vitro reconstitution. *EMBO J.* **15**: 3611–3620.
- STOLER, S., K. C. KEITH, K. E. CURNICK and M. FITZGERALD-HAYES, 1995 A mutation in *CSE4*, an essential gene encoding a novel chromatin-associated protein in yeast, causes chromosome nondisjunction and cell cycle arrest at mitosis. *Genes Dev.* **9**: 573–586.
- STRAIGHT, A. F., A. S. BELMONT, C. C. ROBINETT and A. W. MURRAY, 1996 GFP tagging of budding yeast chromosomes reveals that protein-protein interactions can mediate sister chromatid cohesion. *Curr. Biol.* **6**: 1599–1608.
- STRUNNIKOV, A. V., E. HOGAN and D. KOSHLAND, 1995 *SMC2*, a *Saccharomyces cerevisiae* gene essential for chromosome segregation and condensation, defines a subgroup within the SMC family. *Genes Dev.* **9**: 587–599.
- TAKAHASHI, Y., M. IWASE, M. KONISHI, M. TANAKA, A. TOH-E *et al.*, 1999 Smt3, a SUMO-1 homologue, is conjugated to Cdc3, a component of septin rings at the mother-bud neck in budding yeast. *Biochem. Biophys. Res. Commun.* **259**: 582–587.
- TOTH, A., R. CIOSK, F. UHLMANN, M. GALOVA, A. SCHLEIFFER *et al.*,

- 1999 Yeast cohesin complex requires a conserved protein, Eco1p(Ctf7), to establish cohesion between sister chromatids during DNA replication. *Genes Dev.* **13**: 320–333.
- UHLMANN, F., and K. NASMYTH, 1998 Cohesion between sister chromatids must be established during DNA replication. *Curt. Biol.* **8**: 1095–1101.
- UHLMANN, F., F. LOTTSPREICH and K. NASMYTH, 1999 Sister-chromatid separation at anaphase onset is promoted by cleavage of the cohesin subunit Scc1. *Nature* **400**: 37–42.
- UHLMANN, F., W. WERNEK, M.-A. POUPART, E. KOONIN and K. NASMYTH, 2000 Cleavage of cohesin by the CD clan protease separin triggers anaphase in yeast. *Cell* **103**: 375–386.
- WINZELER, E. A., D. D. SHOEMAKER, A. ASTROMOFF, H. LIANG, K. ANDERSON *et al.*, 1999 Functional characterization of the *S. cerevisiae* genome by gene deletion and parallel analysis. *Science* **285**: 901–906.

Communicating editor: L. PILLUS